ABSTRACT

Dormancy is a strategy observed across all domains of life. *Bacillus subtilis* is a model organism that produces spores that are metabolically dormant. To become metabolically dormant, the *B. subtilis* cell engages in the process of sporulation, which allows bacteria to go on to proliferate even after extermination events that affect a bacteria population. Protein degradation done by AAA+ proteases is a key process in sporulation that prepares the developing spore to become the mature, metabolically inactive spore. Understanding the interactions that trigger the formation and activation of AAA+ proteases within the developing spore is also key to deepening the broader scientific community's understanding of protease function as a whole.

Within *B. subtilis*, the AAA+ protease ClpCP is responsible for cell maintenance, competence development, and spore dormancy progression. The unfoldase component, ClpC, is responsible for recognizing the degron tags of substrates as well as adaptor proteins. Adaptor proteins are proteins that regulate and facilitate interactions between AAA+ proteases and the substrates they target, allowing controlled, event-related protease activity. Novel sporulation specific adaptor protein MdfA is found only in the developing spore, and has recently been shown to activate the ClpCP complex to degrade metabolic enzymes, directly leading to the progression of metabolic dormancy. Current MdfA-ClpC models indicate ClpC and MdfA interact via the ClpC N-Domain with growing evidence of a secondary interaction on the ClpC M-Domain.

The goal of this project was to determine if the ClpC the M-Domain facilitates the *in vivo* function MdfA during the events of sporulation in *Bacillus subtilis*. To accomplish this, we selected a number of mutations to be made along the ClpC M-Domain and in MdfA. We then

measured functions in *B. subtilis* that indicate the MdfA-ClpCP complex was formed during sporulation, as well as outside of sporulation. Through this, we learned that mutations to *mdfA* could disrupt *in vivo* function of MdfA during sporulation, but we were unable to demonstrate the same for mutations made to the *clpC* M-Domain due to pleiotropic effects. However, when measuring *in vivo* function outside of sporulation, mutations to *mdfA* or the *clpC* M-Domain were enough to prevent the formation of MdfA-ClpCP. Furthermore, we were able to restore function by making complementary mutations to both *mdfA* and *clpC*, demonstrating the importance of the ClpC M-Domain in this interaction.

The ClpC M-Domain Facilitates *in vivo* Function of Sporulation Specific Adaptor Protein MdfA in *Bacillus subtilis*

by

Jen Butler

A Paper Presented to the Faculty of Mount Holyoke College

in Partial Fulfillment of the Requirements for

the Degree of Bachelors of Arts with Honor

Program in Biochemistry, South Hadley, MA 01075

May 2025

This paper was prepared

under the direction of

Professor Amy Camp

for eight credits.

ACKNOWLEDGEMENTS

First, I would like to extend my deepest gratitude to my research mentor, Dr. Amy Camp. In a time in my life, and in this country, so fraught with chaos, you have always been by my bench: supporting my research, and reminding me to slow down and appreciate the little (and micro) things in life. You have taught me to be patient, to wait to make my conclusions, to wait to throw out my plates, and I found peace in lab and in the work I was doing. I owe it to you for creating such an amazing environment. You have always embraced all the quirks that I bring to lab and allowed me to carve out a space for myself, where I felt comfortable to thrive. I could not be more grateful for your mentorship, kindness, and joy you have brought to my life in and out of lab.

To my fellow Camp Lab members, past and present, I am grateful to have met you. Jade Morrison, Khushi Panchal, and Chelsea Guo provided critical peer feedback towards this project and made coming to lab a treat. I love the friendships I've built in the Camp Lab with you all and I cannot wait to see all the amazing things we do in the future.

To my wonderful second committee member, Dr. Katie McMenimen, I want to thank you for the expertise you have brought to this project and the support you've given me. I would not have had the confidence to pursue this thesis without the skills you taught me during my time in your classes. You have always been quick to lend a hand to me, in class, in research, and in life. You are the embodiment of the Mount Holyoke spirit and I am so thankful to have met you.

To my fantastic third committee member, Dr. Maria Gomez, I am deeply grateful to have your perspective on this project. I am thankful to have gotten the privilege to have you on my committee, as your curiosity has always encouraged me to dig deeper into the topics I am interested in. Your kindness and wisdom are invaluable to me.

I would also like to thank Dr. Katie Berry and all the Berry Lab members. During my time in Camp Lab, I received expert feedback and comradery from the Berry Lab. Dr. Katie Berry, your direction and honesty was pivotal for this project. You perfectly balance humor with your feedback and you pushed me to refine my research to be the best it can be, thank you.

To my parents, my partner, and to my sweet cat Toblerone, thank you for your enduring love and support. This project has not been an easy one, and it required a great deal of sacrificing time and energy, but you all have continued to love me even when it has not been easy. I love you all very much.

TABLE OF CONTENTS

LIST OF FIGURES

LIST OF TABLES

CHAPTER 1:

INTRODUCTION

1.1 Dormancy is a survival strategy across all domains

An organism's ability to sense, respond, and adapt to its environment is synonymous with an organism's ability to survive. One of the critical ways an organism responds to changes in its environment is by shifting its metabolism. Metabolism is the process by which an organism makes or breaks down complex energy molecules. Any given organism has an energy source that it prefers to draw from, for humans we use glucose as our preferred energy source; however, these resources are not always available to the organism. It might be that an organism has almost exhausted its glucose supply and now needs to slow its consumption of glucose, or switch to using a different energy source. By dialing the rate of metabolism up or down, or by changing the starting or end products of a metabolic pathway, an organism can shift its metabolic strategy to accommodate for changes in the environment.

A more dramatic type of changing metabolic strategies occurs when an organism undergoes a period of metabolic dormancy. Dormancy is a viable state where little to no metabolic activity occurs in the organism for a period of time. This strategy usually occurs in organisms that have evolved to slow their metabolism to outwait harsh environmental conditions. These conditions can range from a lack of available resources, drought, rising or falling temperatures, or another organism has made the environment unlivable. Dormancy strategies are variable between domains but all domains have organisms that engage in a dormancy strategy.

1.1.1 Eukaryotic dormancy strategies

The most famous example of dormancy in eukaryotes is *Ursus americanus*, the American black bear. During the months leading up to winter, black bears increase their caloric intake before undergoing a dormant period known as hibernation. During hibernation, bears are able to switch their metabolic strategy, reducing the amount of calories their bodies burn and recycling urea so they are able to overcome the lack of food characteristic of winter (Barboza 1997).

Other eukaryotic organisms such as *Setaria faberi*, the giant foxtail, use a strategy where the adult organisms produce seeds that are dormant and unable to germinate without the proper environmental triggers. This prevents the seed from attempting to develop during drought periods when it would be unlikely to survive. Upon the right internal and external factors being sensed, metabolism is initiated in the seed, and germination begins (Leon and Owen 2003).

1.1.2 Bacterial dormancy strategies

Many bacteria engage in strategies that involve the formation of a metabolically inactive daughter organism, known as a spore. The spores bacteria form are different from those of eukaryotes. Both are a form of dormant status and usually involve the creation of a cell that is resistant to harsh environment forces that will remain dormant until the right conditions release it. Unlike eukaryotic spores, the spores that bacteria form are not reproductive. Eukaryotic spores, like those of fungi such as yeast, act mainly as a delivery mechanism for an organism's genetic material from one individual to another.

Within the category of spore there are 2 main distinctions: endospore and exospore. To summarize briefly, an exospore is released by budding off from the mother cell where an endospore is produced within the mother cell, which lyses to release the spore. Endospores tend to be stronger and more environmentally resistant structures. Bacteria from the *Bacillus* or *Clostridium* genus are documented for their ability to form endospores.

The most well studied bacteria for spore development is *Bacillus subtilis*, which creates spores during periods of stress and starvation as a survival mechanism. *Bacillus subtilis* is a non-pathogenic, gram-positive bacteria that primarily exists in the soil or in the gut microbiota of mammals. Its safety profile makes it an excellent organism for genetic engineering and developing hypotheses around spore development (See Khanna et al. 2020 for review). This is convenient when trying to build background knowledge that could then be applied to pathogenic bacteria, such as *Clostridiodes difficile* (*C. diff*), that sporulate and are at risk of developing antibiotic resistance (Hota et al. 2012).

1.2 *Bacillus subtilis* Sporulation

The process by which bacteria create spores is known as sporulation. This process is a very taxing one on the cell, and so an individual will take precautionary measures to delay sporulation before it has to begin. In *Bacillus subtilis*, when nutrients start to dwindle and waste builds up, cells will engage in cannibalistic mechanisms to reduce competition with adjacent cells and increase nutrients for themselves (González-Pastor et al. 2003). If enough nutrients are made available, cells will continue to grow vegetatively, where the mother cell divides evenly into 2 bioactive daughter cells. If starvation continues, the vegetative cell undergoes spore formation, beginning with replication of the chromosome (Figure 1). The phases of sporulation can be divided roughly into 3 stages each with key characteristics that may occur overlapping with each other and with other stages (See Tan and Ramamurthi 2014 for review).

1.2.1 The early stages of sporulation

Following the replication of the chromosome, the origin of replication on each chromosome is anchored to opposite ends of the rod-shaped cell by the protein RacA (Ben-Yehuda et al. 2003). During vegetative growth, replication of the chromosome is followed

by the protein FtsZ forming a medial septum known as the Z-ring that constricts and separates the mother cell into 2 equal daughter cells. In contrast, sporulation causes FtsZ to be deployed to the poles of the cell. As a result, the septum forms asymmetrical and creates a larger mother cell and a smaller forespore cell. At the point of asymmetric septum formation, the mother and forespore cell progress through development in a completely different manner. Sigma factors, denoted as σ in this paper, are responsible for these developmental differences, as their presence allows for the transcription of select genes. Certain sigma factors can be active in one compartment but not the other.

Additionally, the septum is built in such a way that the chromosome that is intended to belong to the forespore needs to be transported into the smaller space. The work to push the forespore chromosome into the appropriate space is done by SpoIIIE, a DNA translocase protein, which is localized at the septum midpoint and hydrolyzes ATP to move the chromosome (Wu and Errington 1998). The chromosome, a negatively charged structure that is pushed into a small space, pushes against the septum in a ballooning fashion. Through a combination of natural oscillating movement and the pressure the forespore chromosome generates, the mother cell begins to engulf the forespore, adding an additional membrane layer to the forespore (See Riley et al. 2020 for review).

1.2.2 The middle stages of sporulation

The peptidoglycan that separates the membrane of the mother and forespore is digested partially, while zippering proteins SpoIIQ and SpoIIIAH reach behind the forespore and pinch off the engulfed spore (Meyer et al. 2010). This process leaves the spore free floating in the cytosol of the mother cell. Protein channels that span the membranes of the forespore cell allow flow of metabolic molecules such as amino acids and nucleic acids into the forespore, but not to the mother cell (Camp and Losick 2009; Riley et al. 2021). Metabolism in the forespore slows at

this point, but the forespore still requires metabolic precursors to continue its development. The mother cell is critical in providing not only metabolic precursors for itself, but also for the developing spore. This feeding tube will eventually be cut off as a layer of peptidoglycan and coat proteins form around the engulfed spore (See Riley et al. 2020 for review).

To prepare the spore to survive harsh conditions, the forespore is dressed in a cortex and a coat. The cortex is made of specialized peptidoglycan that is synthesized between the inner forespore membrane and the outer forespore membrane that resulted from mother cell engulfment. The coat forms around the forespore starting back at engulfment and is a layer of several kinds of proteins designed to keep the spore safe (Cutting et al. 1989).

1.2.3 The end stages of sporulation

During this stage, small acid-soluble proteins bind to the forespore chromosome and metabolic activity within the forespore has essentially stopped. This protects the chromosome from damage that could occur by heat, radiation, or oxidative species, while also restricting access to transcription. The mother cell dehydrates the contents of the forespore, allowing the forespore to be resistant to heat (See Riley et al. 2020 for review). Finally, the mother cell lyses and releases the spore into the outside environment. The spore will remain dormant until the right environment conditions have been reached at which point the spore will rehydrate, regain metabolic activity, and regrow.

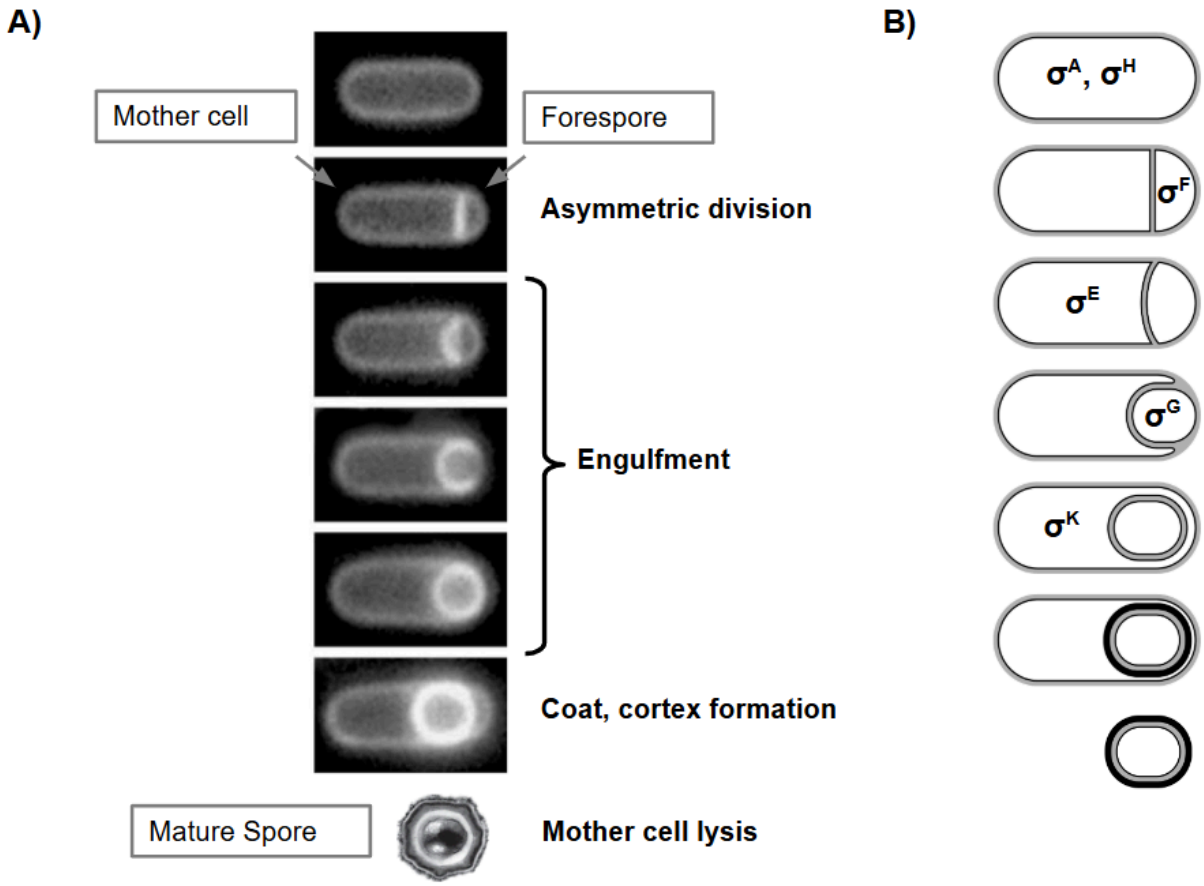

Figure 1. The stages of spore formation, figure made by A. Camp. A) Fluorescent microscopy imaging of the developing spore. The asymmetric septum is highlighted. B) Sigma factors present during the stages of sporulation.

Sporulation is a process that is more extensively studied in terms of protein synthesis pathways; however, there is a growing field of research around protein degradation as it relates to the process of sporulation. In order for the spore to become metabolically dormant, gene expression needs to slow. This can be done in part by restriction of the forespore chromosome and blocking the metabolic precursors coming in from the mother cell, but those alone would not be enough to make the spore dormant in the time frame that is observed (Riley et al. 2021; Riley et al. 2024). Indeed, there is a significant amount of protein degradation that occurs particularly during the middle stages of sporulation done by AAA+ proteases. These proteases are assisted by

adaptor proteins that allow for targeted degradation of metabolic precursors and sigma factors, progressing the spore towards metabolic dormancy.

1.3 ClpCP is a AAA+ Protease

AAA+ proteases (**A**TPases **A**ssociated with diverse cellular **A**ctivities) are characterized by their ability to recognize substrates through degron sequences, interact with adaptor proteins, and hydrolyze ATP to degrade or unfold their substrates. Caseinolytic proteases (Clp) are a family of AAA+ proteases and the primary focus of this paper. AAA+/Clp proteins have been an object of interest in research because of their widespread presence within most bacteria and importance to development (Morreale et al. 2022). Clp proteins tend to oligomerize into stacked ring or barrel-like confirmations with their ATPase domains facing inwards, and substrate recognition domains facing outwards (See Sauer and Baker 2011 for review). Clp proteins are capable of complexing with other Clp proteins that perform different functions. The ClpCP complex is composed of ClpC, a hexamer unfoldase, and ClpP, a two heptameric ring peptidase (Figure 2).

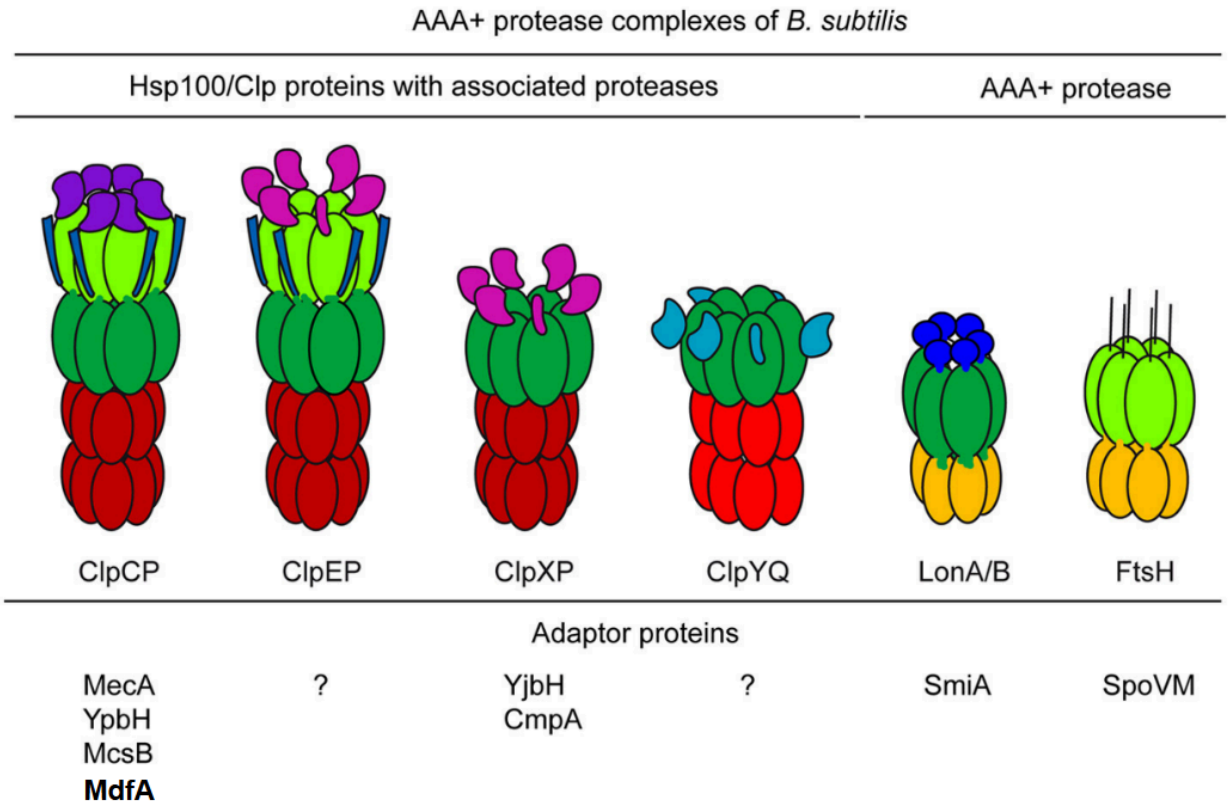

Figure 2. AAA+ proteases within *B. subtilis*. Examples of known adaptor proteins that associate with these proteases are listed respectively, MdfA is a recently discovered ClpCP adaptor. Adapted from Elsholz et al. (2017).

ClpC is found in gram-positive bacteria, as well as some plants, and fulfills roles that are often critical for bacteria survival and development (Annis et al. 2024). Originally, it was thought that ClpC could only unfold substrates with the assistance of adaptor proteins; however, it is now understood that ClpC, and more generally the ClpCP complex, is capable of assembling, identifying substrates, and hydrolyzing ATP to facilitate the restructuring of substrates without adaptor proteins. This occurs at a lower rate than it would with an adaptor protein however.

1.3.1 The role of ClpC within the cell can vary due to presence of sigma factors

The role of ClpC in the cell varies in both when and how it occurs. The *clpC* gene belongs to a larger gene operon called the Class Three Stress Response (CtsR) operon. During

vegetative growth, the CtsR operon, and by extension *clpC*, are expressed at low levels (Schumann 2016); ClpC plays a housekeeping role around the cell, complexing with ClpP and the adaptor protein MecA to handle misfolded or otherwise harmful substrates around the cell that could damage it (Wang et al. 2011). For this role, *clpC* expression is regulated primarily by the presence of σ^A and σ^H. In contrast, during sporulation, ClpC is present in higher amounts, due to σ^F that is present in the forespore, and σ^A, σ^H, and σ^B in the mother cell (Figure 3).

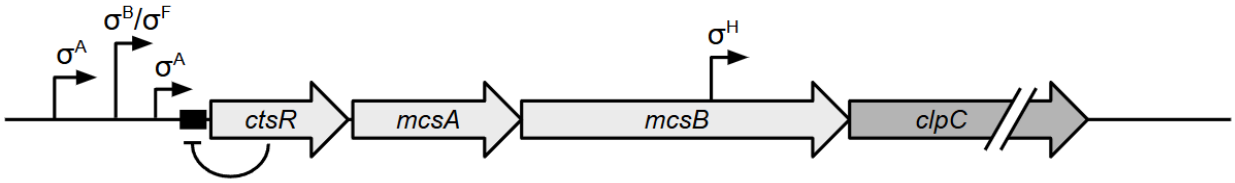

Figure 3. The class three stress response (ctsR) operon map, figure made by A. Camp.

In addition to controlling the amount of ClpC that is present in the cell at any given time, sigma factors also control the amount and kind of adaptor proteins available for ClpC to interact with. Adaptor proteins can cause the assembly or disassembly of the ClpC hexamer and the recruitment of substrates. As an example, during heat stress σ^H is active in higher amounts and causes increased levels of ClpC and the adaptor protein McsB (Nanamiya et al. 1998; Trentini et al. 2016; Schumann 2016). McsB tags misfolded proteins with a phosphorylated arginine (pArg) that the ClpC N-Domain recognizes and unfolds (Kirstein et al. 2007). Under σ^A expression, ClpC and the adaptor protein MecA contribute to the regulation of competence development in *B. subtilis*. MecA binds to the degron sequence of ComK and recruits ClpC to cause unfolding and subsequent degradation, preventing the cell from taking up free DNA at inappropriate times. When the cell senses it's an opportune time to take up DNA, ComS facilitates the release of ComK from MecA-ClpCP by causing the ClpCP complex to disassociate (Turgay et al. 1998).

Before the asymmetric division that occurs during sporulation, ClpC is equally diffused in the cytosol. When the septum forms, the forespore inherits some ClpC from the mother cell. Additionally, the formation of the septum also causes the increase of σ^F in the forespore, which boosts the transcription of the *clpC* gene (Kain et al. 2008; unpublished data from Camp Lab). This high concentration of ClpC in the forespore reduces the forespore's ability to synthesize new substrates and forces the forespore to rely on the mother cell.

1.4 The structure of ClpC plays an important role in the function of ClpC

Within the structure of the ClpC protein monomer there exist 2 domains by which interaction can occur: the amino-terminal N-Domain or the middle M-Domain. Interactions between ClpC and substrates it unfolds occur with the N-Domain. Interactions with adaptor proteins typically occur primarily on the N-Domain and secondarily on the M-Domain (Kirstein et al. 2006). Additionally, the secondary interaction with the M-Domain is not necessarily a shared feature between all ClpC partners. The hexameric structure of ClpC was solved by cryo-EM, using the presence of the adaptor protein MecA (Liu et al. 2013).

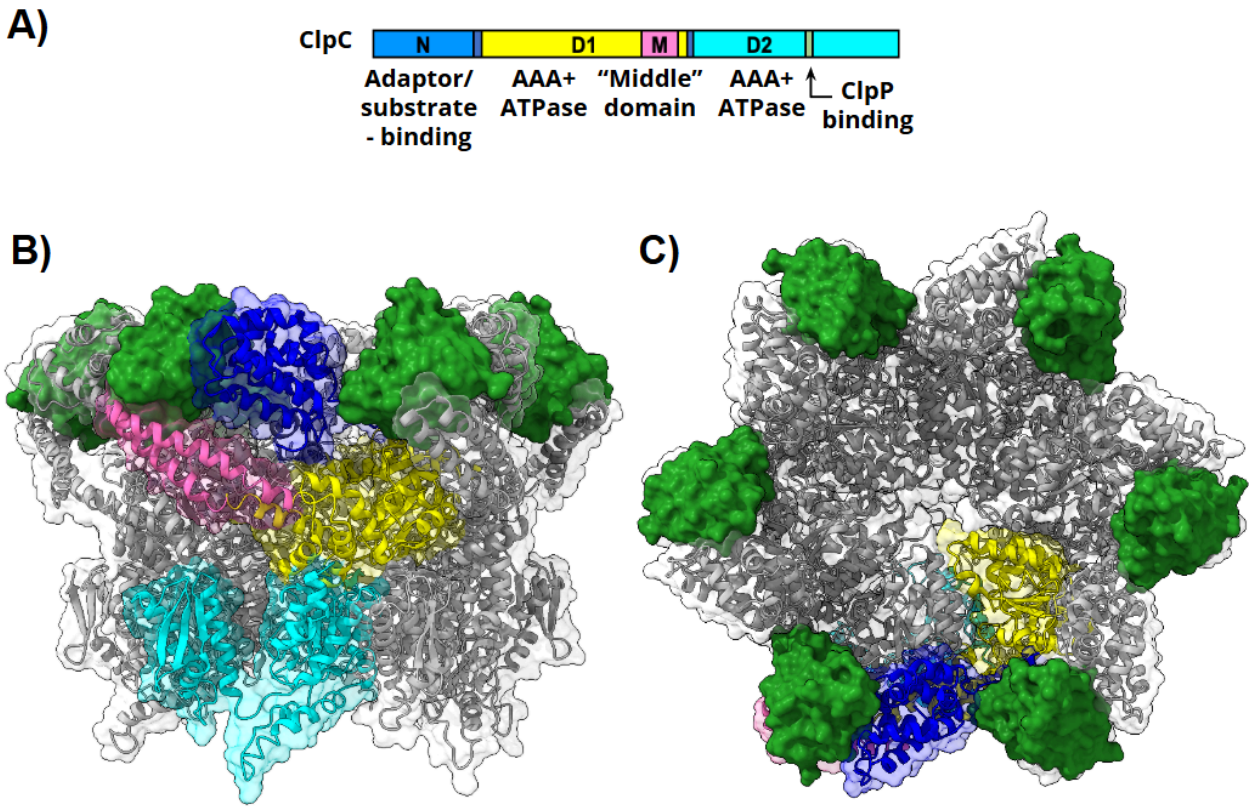

Figure 4. Solved ClpC heximer structure with MecA (Dark green). PBD file (3J3T) from Liu et al. (2013) cryo-EM experiments. Domain colors are mapped onto one ClpC monomer within the full heximer. A) ClpC monomer protein map from A. Camp. B) Side view of ClpC heximer with MecA. C) Top view of ClpC heximer with MecA.

The N-Domain can recognize substrates through the presence of degron tags that are present within the subunit sequence of a substrate (Kuhlmann and Chien 2017). Once a substrate has been recognized directly by the N-Domain or indirectly by an adaptor protein binding to a substrate, it is pulled through the barrel of the ClpC heximer by the hydrolysis of ATP (Trentini et al. 2016). As substrates move through the barrel, first through the D1-Domain then through the D2-Domain, they are forced to unfold (Kirstein et al. 2006). If ClpC is associated with ClpP, the substrate is degraded by peptidase activity (Sauer and Baker 2011).

1.4.1 The M-Domain hold conserved motifs that may be critical to regulation of ClpC

The M-Domain, sometimes referred to as a linker domain, sticks out like an arm from the D1-Domain. The length of the M-Domain varies between genus and species, but within *B. subtilis* the M-Domain is around 55 amino acids long. Within ClpC, the M-Domain appears similar to, but shorter than, the M-Domain that is present on ClpB (Annis et al. 2024). On ClpC and ClpB, the M-Domain appears as a coiled-coil structure made of two adjacent alpha helices. For *B. subtilis*, the tip of the M-Domain is studded in predominantly hydrophobic residues while the middle of the domain has more polar and hydrophilic residues. This is a trend that is common with ClpC homologs with certain residues on the M-Domain being strictly conserved, such as the F436 residue on the tip (Annis et al. 2024).

The current working model for how the M-Domain functions is as a secondary support system to the N-Domain, helping to sandwich or grasp adaptor proteins between the two domains. There are additional theories as to how the M-Domain might perform functions relating to ClpC regulation. It has been shown through cryo-EM of *S. aureus* ClpC, the ClpC M-Domain can form head-to-head interactions with M-Domains on adjacent ClpC molecules (Carroni et al. 2017). This interaction holds ClpC in an inactive state and suggests that the M-Domain could help regulate ClpC activity by preventing oligomerization until there is significant presence of an adaptor protein that breaks the inactive conformation. This phenomenon has not been proved yet in *B. subtilis*.

1.5 The Sporulation Specific Adaptor Protein, MdfA

Metabolic **D**ifferentiation **F**actor **A** (MdfA) is a newly discovered and characterized adaptor protein. It is conserved in aerobic endospore forming bacteria and required for spore

resistance to oxidant forces (Riley et al. 2024). MdfA was found using genetic screening, where, when the *mdfA* gene was knocked out, gene expression controlled by σ^F in the forespore subsequently increased (Massoni and Evans et al. 2025). Additionally, it was determined that *mdfA* was only present in the forespore, and under the expression of σ^F following asymmetric division. This led to a model where the *in vivo* function of MdfA is to oligomerizer with ClpC and progress a negative feedback loop (Figure 5).

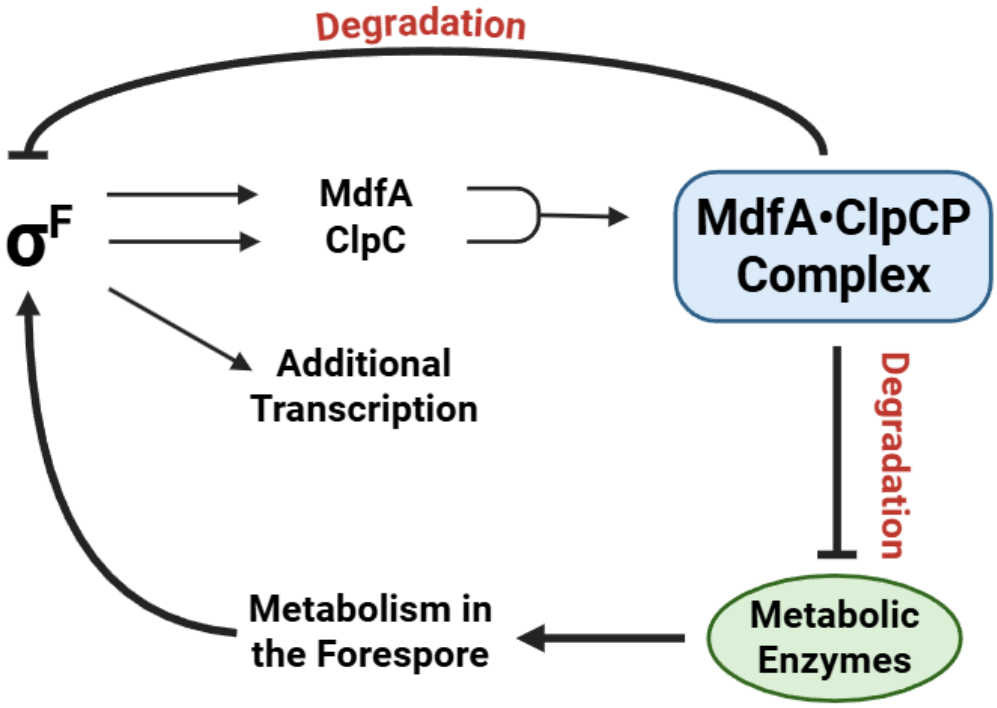

Figure 5. σ^F related activity in the forespore leads to a negative feedback loop where the transcription of *clpC* and *mdfA* causes decreased levels of σ^F in the developing spore. Figure made using BioRender.

The presence of σ^F in the forespore leads to the transcription of *mdfA* and *clpC* that then oligomerize and cause degradation of metabolic enzymes and of σ^F in the forespore (Pan et al. 2001; Riley et al. 2024). This both directly and indirectly reduces the amount of σ^F related activity that occurs in the forespore and allows for the transition from σ^F to σ^G related activity,

progressing the cascade of gene expression (Kroos et al. 1999; Massoni et al. 2025). Interestingly, despite the role MdfA plays in metabolic shutdown in the forespore, the removal of *mdfA* did not impact counts of heat resistant spores.

MdfA structure is conserved among the *Bacillaceae* family and it does not appear to have any ATPase capable domains (Riley et al. 2024). It was determined that MdfA acts as an adaptor protein to ClpC because of observations made by selectively mutating single residues in the *clpC* N-Domain region and observing the same break in the negative σ^F feedback loop characteristic of the MdfA-ClpCP complex not being present to degrade σ^F (Massoni et al. 2025). This was then demonstrated further in a B2H assay that measured interactions between the domains of ClpC with MdfA, where it was shown that the ClpC N-Domain was sufficient to report interaction between ClpC and MdfA. Interestingly, from that same investigation, it was seen that, while the N-Domain alone was sufficient to produce interaction, the interaction was stronger when the N-Domain and D1M-Domain were both present.

1.5.1 Preliminary evidence for ClpC M-Domain and MdfA interaction

With the B2H assay pointing to the importance of the inclusion of the M-Domain for the MdfA-ClpC interaction, the protein structure prediction software AlphaFold was utilized by collaborators in the Carroni lab to visualize how MdfA-ClpC could look like. AlphaFold uses data from cryo-EM measurements taken between ClpC and MecA to then model how MdfA-ClpC could interact (See Evans et al. 2022 for review). The model was adjusted by the inclusion of parameters that MdfA and ClpC interact definitely on the N-Domain. The result was a prediction that had MdfA coming in contact with the M-Domain of ClpC, in addition to the N-Domain.

1.6 A genetic approach to determining the ClpC^{MD}-MdfA interaction

While cryo-EM is an excellent tool for determining protein structure and function, it is less of an option for proving the ClpC^{MD}-MdfA interaction for two main reasons: oligomerized ClpCP and MdfA are not symmetrical, and we are interested in determining if the ClpC^{MD}-MdfA interaction occurs *in vivo*. Fellow lab collaborator Jade Morrison and I approached this project from two angles. Morrison used genetic manipulation in the *E. coli* based Bacterial-2-Hybrid (B2H) assay (See Discussion) to measure *B. subtilis* ClpC-MdfA interactions. I aimed to genetically manipulate *B. subtilis* to measure these same protein interactions during sporulation.

We hypothesized that the ClpC M-Domain facilitates the *in vivo* role of MdfA in *B. subtilis* during sporulation. To test this, we made mutations to the native *clpC* and *mdfA* genes in codons for residues predicted to be at the interface of the ClpC M-domain and MdfA interaction. We then assessed functions relating to the negative σ^F feedback loop using a σ^F-proxy β-galactosidase activity assay. Additionally, we assessed the *in vivo* function of MdfA-ClpC outside of sporulation using an IPTG-inducible MdfA toxicity assay. Through these methods, we found that the importance of M-Domain interaction for MdfA *in vivo* function could be proved during sporulation through mutations to *mdfA*, and proven outside of sporulation through mutations to *clpC* or *mdfA*. In short, we are moving towards a model of MdfA-ClpC that involves the interaction of both the ClpC N-Domain and M-Domain to allow for the *in vivo* function of MdfA during *B. subtilis* sporulation.

CHAPTER 2:

MATERIALS AND METHODS

2.1 Site-Directed Mutagenesis

2.1.1 Development of Site-Directed Mutagenesis Primers

Primers were developed using guidelines outlined by Liu and Naismith (2008) for efficient single-site mutations to plasmids. To summarize, primer pairs are designed with a longer non-overlapping sequence at the 3' end and a shorter overlapping sequence at the 5' end. Forward primers (F) were designed to include the desired mutation 1 base away from the overlapping region. Reverse primers (R) were designed not to include any mutations. Newly synthesized PCR product containing the desired mutation acts as the new template for subsequent rounds of PCR, leading to amplification of mutated plasmid.

2.1.2 Q5® High-Fidelity

To create a point mutation at the target site, a Q5® High-Fidelity 2X Master Mix developed by New England Biolabs Inc. (Catalog# M0492S) was used. NEB recommended PCR protocol was followed. Forward and reverse primers were designed by Dr. Amy Camp using NEBase Changer® (See Table 1 for primer details). PCR reactions were generally set up as follows: A final concentration of ~10 ng/μL of template plasmid, 10 μM of forward and reverse primer, and 1X of Q5® High-Fidelity 2X Master Mix (containing DNA polymerase, buffer, and dNTPs). Thermocycling conditions varied (See Table 2 for details on plasmid conditions), but in general an initial denaturation at 98ºC occurred for 30 seconds, followed by 18-25 cycles consisting of denaturation at 98ºC for 10 seconds, primer annealing 65ºC for 30 seconds, and

extension at 72°C for 45 seconds per kb of template plasmid. Final extension was held at 72°C for 5 minutes.

Table 1. Oligonucleotides used for this study

Primer name	Sequence (5' → 3')	Purpose
oAC46	TTG GCT ACT GGT ACA CA**G** **C**GT GGA ATC CGC ATA TGT ATG AAC AAA TC	mdfA E190A F
oAC47	TTG GCT ACT GGT ACA CA**A** **AG**T GGA ATC CGC ATA TGT ATG AAC AAA TC	mdfA E190K F
oAC48	TTG GCT ACT GGT ACA CA**A** **GG**T GGA ATC CGC ATA TGT ATG AAC AAA TC	mdfA E190R F
oAC49	TGT GTA CCA GTA GCC AAT TTC CGC TCG GTT TTT CAG C	mdfA E190 R
oAC50	ATG AGG TTC GTA AAG AG**G** **C**GG ATG CGG CAG TGC AAA G	clpC K427A F
oAC51	ATG AGG TTC GTA AAG AG**G** **AG**G ATG CGG CAG TGC AAA G	clpC K427E F
oAC52	CTC TTT ACG AAC CTC ATC AAG CTT CTG CTC AAG CTC	clpC K427 R
oAC53	AAA AAG CTG CTT CCT TG**G** **C**TG ATA CTG AAC AAC GCC TGC G	clpC R443A F
oAC54	AAA AAG CTG CTT CCT TG**G** **AG**G ATA CTG AAC AAC GCC TGC G	clpC R443E F
oAC55	CAA GGA AGC AGC TTT TTC AAA CTC TTG GCT TTG CAC TGC	clpC R443 R
oFQ1	ATC GCT GGG TAG CTA TGT GCG	Amplify ΔctsR F
prSM56	CAG AAT GAG AAA AAG CCG CTC TCC G	Amplify ΔctsR R
prRS6	ACA TAA CCC GGA GGT GAA CC	Sanger Sequencing mcsB-clpC region F

Table 2. Site Directed Mutagenesis Reactions

Template plasmid	Desired Mutation	Primer Pair	Annealing Temperature (°C)	Resulting Plasmid
pSM26	E190R in *mdfA*	oAC48, oAC49	65	pJB1
pSM26	E190K in *mdfA*	oAC47, oAC49	65	pJB2
pSM26	E190A in *mdfA*	oAC46, oAC49	65	pJB3
pSY1	E190A in *mdfA*	oAC46, oAC49	65	pJB4
pSY1	E190K in *mdfA*	oAC47, oAC49	65	pJB5
pSY1	E190R in *mdfA*	oAC48, oAC49	65	pJB6
pAH742	K427A in *clpC*	oAC50, oAC52	72	pJB7
pAH742	R443A in *clpC*	oAC53, oAC55	72	pJB8
pAH742	K427E in *clpC*	oAC51, oAC52	72	pJB9
pAH742	R443E in *clpC*	oAC54, oAC55	72	pJB10

2.2 *B.subtilis* strain construction

2.2.1 Creation of mutations in the native chromosome at *clpC* locus

For mutations made to the *B.subtilis mdfA* gene, a plasmid containing a modified *mdfA* gene and a CRISPR-*Cas9* cassette was used (See Table 3 for details on plasmids used). The plasmid was then inserted into a *B.subtilis* strain containing a *mdfA* knockout and grown at room temperature on LB/Kan15/0.2% Mannose containing plates. Successful colonies were restruck onto LB/Kan15/0.2% Mannose plates an additional 2 times before candidates were struck onto LB agar and grown at 45°C overnight to remove CRISPR-*Cas9* plasmid. This process was repeated about 6 times to ensure the plasmid had left *B.subtilis*.

For mutations made to the *B.subtilis clpC* gene, due to the necessity of *clpC* for development of competence, strains containing a *clpC* knockout could not be used to mutate the

native chromosome. Instead, a plasmid containing adjacent *clpC* genes (*mcsA-mcsB-clpC-radA*) and a CRISPR-*Cas9* cassette was first mutated to contain a modified *clpC*. The plasmid was then inserted into a *B.subtilis* strain containing a *mcsB* knockout. To favor the chances of recombination occurring downstream of where the desired mutation in *clpC* was, more homologous DNA downstream of *mcsB*, *clpC-radA* region, was included.

Successfully mutated plasmids containing repair template, appropriate guide RNA and *cas9* cassette were transformed into NEB® 10-beta Competent *E. coli* (New England BioLabs Inc., Catalog# C3019H) by heat shocking at 42ºC for 30 seconds and growing on an appropriate antibiotic selection plate overnight at 37ºC.

Single colonies from selection plates were inoculated into 2 mL of LB containing the same selection antibiotic and grown overnight in an incubator at 37ºC. Cultures were then miniprepped using a modified NucleoSpin® Plasmid/Plasmid: Isolation of high-copy plasmid DNA from *E. coli* protocol. Isolated and verified plasmids were then transformed into JBB36 (see Table 4 for strain construction) following the "(Very Easy) One Step *Bacillus subtilis* Transformation" protocol in the Camp Lab up until the addition of plasmid (see Section 2.2.2 for details). 5 µL of plasmid was inserted into 200 µL of competent *B. subtilis* strain culture and allowed to grow at 37ºC for 1 hour.

A modified procedure using guidelines developed by Sachla et al. (2021) for engineering *B.subtilis* using CRISPR-*Cas9* was used. Transformed strains were spread on antibiotic selection plates containing 0.2% mannose, adjusted for *B. subtilis* sensitivities, and growth at 25ºC overnight. Single colony candidates were selected and struck onto selection plates containing mannose then grown overnight at 25ºC. Candidates were subsequently repatched onto LB agar and grown at 45ºC overnight, this step was repeated 4-5 times until candidates became sensitive

to Kan_5 and MLS. 4 Candidates were struck for single colonies on LB agar, then 4 single colonies from each candidate was patched to test for Kan_5 and MLS sensitivity indicating loss of plasmid and successful repair.

Chromosomal DNA isolation was performed on successful candidates (See Section 2.3 for more details) and amplified with PCR using primers oFQ1 and prSM56 (Table 1). PCR products were cleaned using Monarch® PCR & DNA Cleanup Kit (New England Biolabs Inc., Catalog# T1130L) following the PCR cleanup protocol provided in the user manual.

PCR products were sent for initial confirmation by Sanger sequencing using primer prRS6 (Table 1), candidates containing the mutation of interest and no other obvious mutations were selected for nanopore sequencing. Verified strains were saved in duplicate as frozen stocks at -80ºC in 20% glycerol.

2.2.2 Transformation of plasmids into a *B.subtilis* recipient strain

The desired *B. subtilis* recipient strain was inoculated into a 1X Modified Competence (MC) medium (14.04 mg/mL $K_2HPO_4 \cdot 3H_2O$, 5.24 mg/mL KH_2PO_4, 20.00 mg/mL glucose, 0.88 mg/mL trisodium citrate, 0.02 mg/mL ferric ammonium citrate, 1.00 mg/mL casein hydrolysate, 2.00 mg/mL potassium glutamate, 0.24 mg/mL $MgSO_4 \cdot 7H_2O$, and deionized water) and was incubated for 4 hours at 37ºC on a roller drum. The appropriate donor plasmid was transferred to 200 µL of cell culture and allowed to continue growing for 1 hour at 37ºC on a roller drum. Samples were plated onto LB plates containing an appropriate selection antibiotic to control for successful integration of plasmid. Independent single colonies were selected to be restruck onto a selection plate to ensure continued resistance against appropriate antibiotics. Candidates were selected to be repatched onto LB plates containing 10 mg/mL of potato starch and grown overnight at 37ºC. Patches were then exposed to an iodine solution to ensure insertions at the

native *amyE* site. Successfully constructed strains containing the desired mutations were stored as frozen stocks at -80ºC in 20% glycerol.

2.3 Isolation of *B.subtilis* Chromosomal DNA

To isolate *B. subtilis* chromosomal DNA, a Promega Wizard® modified protocol for "3.G. Isolating Genomic DNA from Gram Positive and Gram Negative Bacteria" from the user manual is used.

A single colony from the desired *B. subtilis* strain was inoculated into 3 mL of LB liquid and grown on a roller drum for 3 hours at 37ºC. 2 mL of the liquid culture was then spun at 13,000 rcf for 2 minutes and the supernatant liquid was removed (cell pellets were occasionally stored at -20ºC at this stage). Cell pellets were resuspended thoroughly in 480 µL of 50 mM EDTA then 30 µL of 20 mg/mL of lysozyme was added to samples and inverted to mix. Samples were incubated at 37ºC for 45 minutes and then 600 µL of Nuclei Lysis Solution (purchased from Promega, Catalog# A7941) was gently pipetted in. Samples were incubated at 80ºC for 5 minutes to lyse cells, then allowed to cool to room temperature. 3 µL of 4 mg/mL RNase solution was added to samples and then incubated at 37ºC for 45 minutes. Samples were cooled to room temperature before 200 µL of Protein Precipitation Solution (purchased from Promega, Catalog# A7951) was added to the RNase-treated lysate and vortexed at high speed for 20 seconds. Samples were incubated on ice for 5 minutes, then centrifuged at 13,000 rcf for 3 minutes. 900 µL of supernatant was transferred to a microcentrifuge tube containing 600 µL of room temperature isopropanol. The samples were then inverted gently to mix and centrifuged at 13,000 rcf for 2 minutes. All supernatant liquid was pipetted from the tube and the chromosomal DNA pellet was allowed to dry under the fume hood for 45 minutes. The chromosomal DNA

pellet was then rehydrated with 100 µL of Elution Buffer overnight at room temperature. Once rehydrated, samples were stored at -20ºC.

2.4 Spore Efficiency Assay

Spore efficiency was determined using a modification of methods described previously (Mearls et al. 2018). A single colony from the desired *B. subtilis* strain was inoculated into 2 mL of Difco Sporulation Media (DSM) with supplements (100 µL $FeSO_4$ stock solution, 0.0952 mg/mL $MnCl_2$, 16.41 mg/mL $Ca(NO_3)_2$) to induce sporulation via nutrient exhaustion, and incubated at 37ºC for 24 hours. After incubation, samples were placed in an 80ºC water bath for 20 minutes, and 10-fold serial dilutions were performed until the desired dilution was reached. 100 µL of sample was spread on a plate containing DSM and allowed to grow overnight at 37ºC. Following this, single colonies were counted. Colony counts exceeding 300 and below 10 weren't counted. To calculate spore efficiency, the number of single colonies was multiplied by its dilution factor, then divided by the volume of sample plated.

2.5 β-galactosidase Assay

2.5.1 Induction of Sporulation by Resuspension

To collect samples at different sporulation stages, a modified protocol for the "Induction of sporulation by the resuspension method" from Section 9.2.2.c of Hardwood and Cutting *Molecular Biological Methods for Bacillus* was used.

A single colony of the desired *B. subtilis* strain containing a σ^F-inducible lacZ gene was inoculated into 5 mL of a rich medium (CH) and grown for 3 hours at 37ºC until OD600 readings reached the range of 0.5 - 0.8, indicating cultures were within the exponential growth phase. OD600 values were recorded and cultures were diluted into 20 mL of CH media to an

OD600 value of 0.05. Samples were then cultured in a 37ºC water bath shaker for 2.5 hours until an OD600 value within the range of 0.5 - 0.8 is reached. Samples were then spun down at 3220 rcf for 10 minutes at room temperature and supernatant liquid was poured off. The cell pellet was subsequently resuspended in 20 mL of A+B Sporulation Media and transferred back to its original culturing flask in the 37ºC water bath. 1 mL of the sample was saved and centrifuged at 21300 rcf for 1 minute, supernatant liquid was aspirated off and samples were stored at -80ºC. This was repeated every hour until 6 time points were collected.

2.5.2 Kinetic β-galactosidase Assay

To measure enzyme activity in collected *B. subtilis* samples, a protocol developed by Dr. Amy Camp, see Camp and Losick (2009) *Genes Dev* 23:1014, was used. This protocol was modified to account for increased enzyme activity of strains that had boosted gene expression.

Cell pellets were resuspended in 500 µL Z-buffer (60.1 mM $Na_2HPO_4 \cdot 7H_2O$, 39.86 mM $NaH_2PO_4 \cdot H_2O$, 10.1 mM KCl, 0.974 mM $MgSO_4 \cdot 7H_2O$)/βME solution and OD600 values were recorded. A solution of Lysozyme in Z-Buffer was prepared (0.267 mg/mL lysozyme) and 75 µL of solution was transferred to 25 µL of cell resuspension in a 96 well-plate. The sample plate was then incubated at 37ºC for 25 minutes to lyse cells. 20 µL of ONPG in Z-Buffer (4 mg/mL ONPG) warmed to 37ºC was added to the sample plate and OD420 was read every minute for 1 hour at 37ºC.

OD420 values above 0.75 OD and points taken during the first 10 minutes were masked. To calculate β-galactosidase activity, the mean maximum velocity (V_{max}) for each well representing a point in time during sporulation was divided by its corresponding OD600 value.

2.6 IPTG induced-MdfA Toxicity Assay

To determine toxicity phenotype, a modified procedure using methods described in "MdfA is a novel ClpC adaptor protein that functions in the developing *Bacillus subtilis* spore" from Massoni et al. (2025), was used.

A single colony from the desired *B. subtilis* strain was inoculated into 3 mL of LB media and incubated for 6 hours at 37°C. 200 µL of undiluted culture was transferred to a 96 well-plate, then 20 µL of undiluted culture was diluted into a well containing 180 µL of sterile water, this was repeated until the desired final dilution is reached. A metal "frogger" was flame sterilized and allowed to cool before being dipped into culture containing wells and stamped first on an LB plate, then a plate containing 1 mM of IPTG. Plates were grown at room temperature for 48 hours and then imaged. Following initial documentation, plates were imaged every 24 hours up to an additional 72 hours.

Table 3. Plasmids used for this study

Plasmid	Description	Selection	Source or Construction
For β-galactosidase Assay			
pAH136	*amyE*::P_{spoIIQ}-*lacZ cm*, *amp*	CM (Bs), AMP (Ec)	Camp and Losick 2009
For Toxicity Assay			
pSM26	*amyE*::$P_{hyperspank}$-*mdfA lacI spc*, *amp*	SPT (Bs), AMP (Ec)	Massoni et al. 2024
pJB1	*amyE*::$P_{hyperspank}$-*mdfA*(E190R) *lacI spc*, *amp*	SPT (Bs), AMP (Ec)	Site-directed mutagenesis of pSM26 with oAC48 and oAC49.
pJB2	*amyE*::$P_{hyperspank}$-*mdfA*(E190K) *lacI spc*, *amp*	SPT (Bs), AMP (Ec)	Site-directed mutagenesis of pSM26 with oAC47 and oAC49.

pJB3	*amyE*::$P_{hyperspank}$-*mdfA*(E190A) *lacI spc*, *amp*	SPT (Bs), AMP (Ec)	Site-directed mutagenesis of pSM26 with oAC46 and oAC49.
For CRISPR Modification			
pSY1	*mdfA* repair template in pAJS23 (ori[ts] cas9 erm-gRNA kan)	KAN (Bs)	Built by Siyu using pAJS23 gifted from Helmann lab, Sachla et al. 2021
pJB4	*mdfA*(E190A) repair template in pAJS23	KAN (Bs)	Site-directed mutagenesis of pSY1 with oAC46 and oAC49
pJB5	*mdfA*(E190K) repair template in pAJS23	KAN (Bs)	Site-directed mutagenesis of pSY1 with oAC47 and oAC49
pJB6	*mdfA*(E190R) repair template in pAJS23	KAN (Bs)	Site-directed mutagenesis of pSY1 with oAC48 and oAC49
pAH742	mcsB-clpC repair template in pAJS23	KAN (Bs)	Camp Lab Stock, made by A. Camp
pJB7	*clpC*(K427A) repair template in pAJS23	KAN (Bs)	Site-directed mutagenesis of pAH742 with oAC50 and oAC52.
pJB8	*clpC*(R443A) repair template in pAJS23	KAN (Bs)	Site-directed mutagenesis of pAH742 with oAC53 and oAC55.
pJB9	*clpC*(K427E) repair template in pAJS23	KAN (Bs)	Site-directed mutagenesis of pAH742 with oAC51 and oAC52.
pJB10	*clpC*(R443E) repair template in pAJS23	KAN (Bs)	Site-directed mutagenesis of pAH742 with oAC54 and oAC55.

Table 4. *B.subtilis* strains used or constructed for this study

Strain	Genotype	Source or Construction

PY79 (JBB1)	Prototrophic wild type	Youngman et al. 1984
CFB270 (JBB2)	Δ*clpC*::erm	Massoni et al. 2024
SOB7 (JBB5)	*clpC*(F436A)	Camp Lab Stock, made by S. Obwar and R. Fekade
SMB251 (JBB8)	Δ*mdfA*::*erm*	Massoni et al. 2024
JBB9, 10	*clpC*(F436A), *amyE*::$P_{hyperspank}$-*mdfA lacI spc*	pSM26 → JBB5
CFB189 (JBB11)	*amyE*::$P_{hyperspank}$-*mdfA lacI spc*	Massoni et al. 2024
CFB241 (JBB12)	Δ*clpC*::*erm*, *amyE*::$P_{hyperspank}$-*mdfA lacI spc*	Massoni et al. 2024
JBB14, 15	*clpC*(F436A) *amyE*::P_{spoIIQ}-*lacZ cm*	pAH136 → JBB5
AHB881 (JBB18)	*amyE*::P_{spoIIQ}-*lacZ cm*	Camp and Losick 2009
SMB189 (JBB19)	Δ*mdfA*::*erm*, *amyE*::P_{spoIIQ}-*lacZ cm*	Massoni et al. 2024
JBB20	Δ*clpC*::*erm*, *amyE*::P_{spoIIQ}-*lacZ cm*	Massoni et al. 2024
JBB21, 22	*amyE*::$P_{hyperspank}$-*mdfA*(E190R) *lacI spc*	pJB1 → JBB1
JBB23, 24	*amyE*::$P_{hyperspank}$-*mdfA*(E190K) *lacI spc*	pJB2 → JBB1
JBB25, 26	*amyE*::$P_{hyperspank}$-*mdfA*(E190A) *lacI spc*	pJB3 → JBB1
JBB27, 28, 29	*mdfA*(E190A) *amyE*::P_{spoIIQ}-*lacZ cm*	pJB4 → JBB19
JBB30, 31, 32	*mdfA*(E190K) *amyE*::P_{spoIIQ}-*lacZ cm*	pJB5 → JBB19
JBB33, 34, 35	*mdfA*(E190R) *amyE*::P_{spoIIQ}-*lacZ cm*	pJB6 → JBB19
JBB36	Δ*mcsB*::*erm*	Camp Lab Stock, made by F. Quigley 2023
JBB38, 39	*clpC*(F436A), Δ*mdfA*::*erm*, *amyE*::P_{spoIIQ}-*lacZ cm*	JBB19 chDNA → JBB14
JBB40, 41	*clpC*(K427A)	pJB7 → JBB36

JBB42, 43	*clpC*(R443A)	pJB8 → JBB36
JBB44, 45	*clpC*(K427E)	pJB9 → JBB36
JBB46, 47	*clpC*(R443E)	pJB10 → JBB36
JBB48, 49	*clpC*(K427A), *amyE*::$P_{hyperspank}$-*mdfA lacI spc*	pSM26 → JBB40
JBB50, 51	*clpC*(R443A), *amyE*::$P_{hyperspank}$-*mdfA lacI spc*	pSM26 → JBB42
JBB52, 53	*clpC*(K427E), *amyE*::$P_{hyperspank}$-*mdfA lacI spc*	pSM26 → JBB44
JBB54, 55	*clpC*(R443E), *amyE*::$P_{hyperspank}$-*mdfA lacI spc*	pSM26 → JBB46
JBB56, 57	*clpC*(K427A), *amyE*::P_{spoIIQ}-*lacZ cm*	pAH136 → JBB40
JBB58, 59	*clpC*(R443A), *amyE*::P_{spoIIQ}-*lacZ cm*	pAH136 → JBB42
JBB60, 61	*clpC*(K427E), *amyE*::P_{spoIIQ}-*lacZ cm*	pAH136 → JBB44
JBB62, 63	*clpC*(R443E), *amyE*::P_{spoIIQ}-*lacZ cm*	pAH136 → JBB46
JBB68, 69	*clpC*(K427E), *amyE*::$P_{hyperspank}$-*mdfA*(E190K) *lacI spc*	pJB2 → JBB44
JBB70, 71	*clpC*(R443E), *amyE*::$P_{hyperspank}$-*mdfA*(E190R) *lacI spc*	pJB1 → JBB46

CHAPTER 3:

RESULTS

3.1 Identification of side chain candidates important to ClpC-MdfA interaction for mutagenesis

To determine the necessity of the ClpC M-Domain for *in vivo* MdfA function during sporulation, I started by searching along the M-Domain and MdfA for residues that might be important for the $ClpC^{MD}$-MdfA interaction. I reasoned that by creating a collection of residues to target for mutation on ClpC and MdfA that were expected to break the interaction, I could measure resulting phenotypes to determine MdfA's *in vivo* function. To perform my search, I utilized AlphaFold predictions performed by collaborators in the Carroni Lab. These predictions were visualized using ChimeraX to generate a potential model interaction between a ClpC monomer and MdfA. Crystallography is unable to visualize hydrogen bonding between side chains but AlphaFold and ChimeraX use artificial intelligence models to determine where intramolecular interactions could occur.

One residue that stood out initially was the F436 residue that sits at the tip of the M-Domain and is predicted to interface with residues on MdfA (Figure 6B). An additional reason why this residue stuck out was because within our lab collection, we already possessed a *clpC*^{F436A} mutant. Furthermore, F436, as well as R443, has documented importance for adaptor protein interactions and is well conserved across ClpC homologs (Massoni et al. 2025).

While exploring the ChimeraX model, I started with looking at R443 on ClpC, as it was highlighted by Carroni et al. 2017. I noted that R443, a positively charged arginine residue, is

predicted to share a hydrogen bond with the carbonyl backbone of E190, a negatively charged glutamic acid, on MdfA. Additionally, the E190 residue is highly conserved within the *Bacillaceae* family (Massoni et al. 2025). The proximity between R443 and E190 made me curious if the two shared an electrostatic interaction.

The salt bridge between R443 and E190 then led me to find K427, lysine, another positively charged residue, which ChimeraX predicted to share 2 potential hydrogen bonds with E190 on MdfA. Additionally, similar to R443, K427 seemed to be proximal enough to E190 to share an electrostatic interaction. With the limited area of interaction between $ClpC^{MD}$ and MdfA, the theoretical interaction of 2 positively charged residues on ClpC sandwiching a negatively charged residue on MdfA was a good place to start mutating to determine the importance of the $ClpC^{MD}$-MdfA interaction.

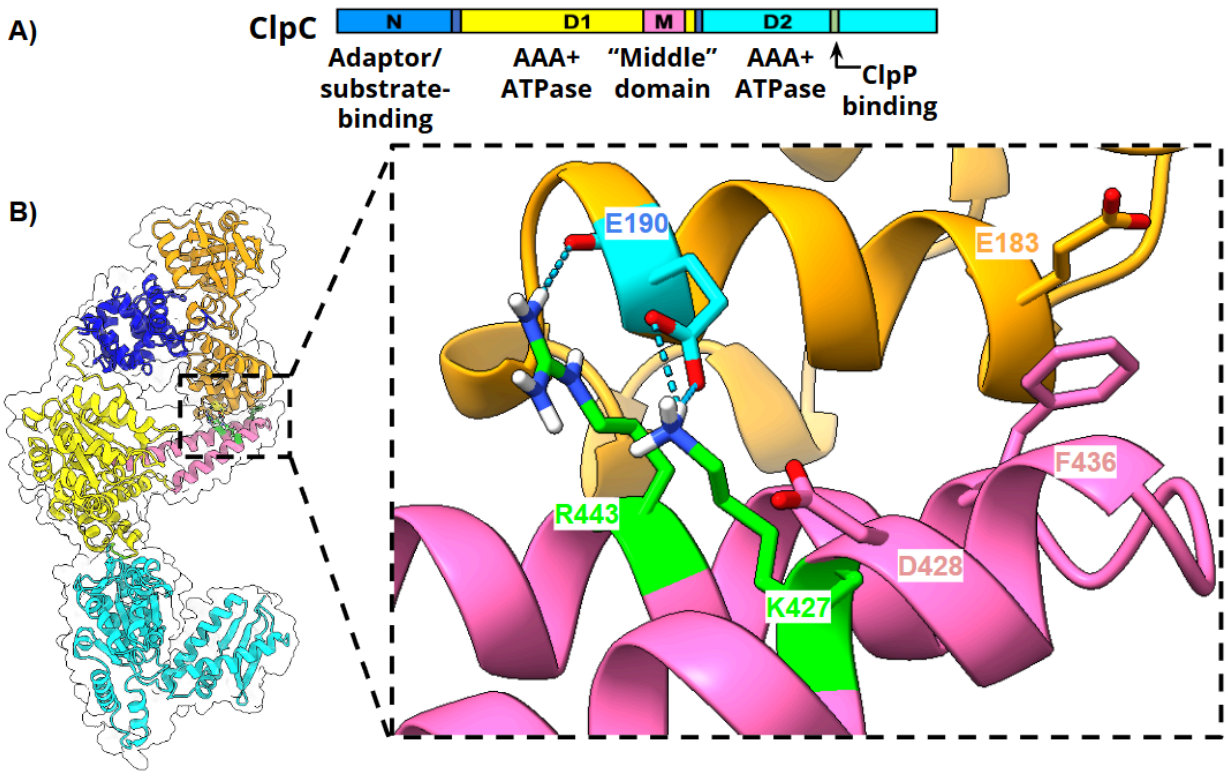

Figure 6. A) Domain structure of the ClpC protein monomer, made by A. Camp. Shown are the adaptor/substrate binding N-Domain (dark blue), AAA+ ATPase D1-Domain (yellow), middle/linker M-Domain (pink), and AAA+ ATPase D2-Domain (cyan). The ClpP binding site within the D2-Domain is shown in gray. B) ChimeraX visualization of AlphaFold prediction of ClpC monomer with MdfA (unpublished work from collaborators in the Carroni Lab). ClpC M-Domain is predicted to come in contact with MdfA. New identified residues on M-Domain suspected to have importance in MdfA-ClpC interaction are highlighted in green if on ClpC or cyan if on MdfA.

Once residues were identified, I proceeded to use a CRISPR/Cas9 system to mutate the corresponding codons within the native *B.subtilis clpC* and *mdfA* gene. There were 3 versions of E190 created: $mdfA^{E190A}$, $mdfA^{E190K}$, and $mdfA^{E190R}$. In addition, I created 2 versions each of R443 and K427: $clpC^{R443A}$, $clpC^{R443E}$, $clpC^{K427A}$, and $clpC^{K427E}$.

3.1.2 Creating mutations to the native *clpC* and *mdfA* genes in *B. subtilis*

To summarize, a plasmid containing the Cas9 gene, guide RNA, and homologous DNA with a mutant gene that will repair the cut area, is inserted into a strain that contains a knockout

(replaced with an antibiotic resistance gene, *erm*) of the desired gene for mutagenesis. The plasmid is transcribed with the presence of mannose. Cas9, associated with the *erm* guide RNA, creates a double stranded break in the native chromosome of *B. subtilis*. This break is then repaired using homologous recombination that replaces the *erm* resistance gene with a mutant version of the native gene.

This method was used for creating mutations to the native *mdfA* gene in *B. subtilis*; however, this method could not be used for mutating *clpC*. As discussed, ClpC is an important regulator of *B. subtilis* competence, meaning we could not induce competence with a *B. subtilis* strain without ClpC, and therefore could not insert the CRISPR/Cas9 plasmid. To get around this, we used a different method for mutating *clpC* described by Sachla et al. (2021). To summarize, we started with a strain that lacks the adjacent, upstream gene of *clpC*, *mcsB*. Recombination can occur anywhere along the chromosome and plasmid where there is homologous DNA; to increase the likelihood that the mutation on *clpC* is taken up, we included more homologous DNA downstream of *mcsB*.

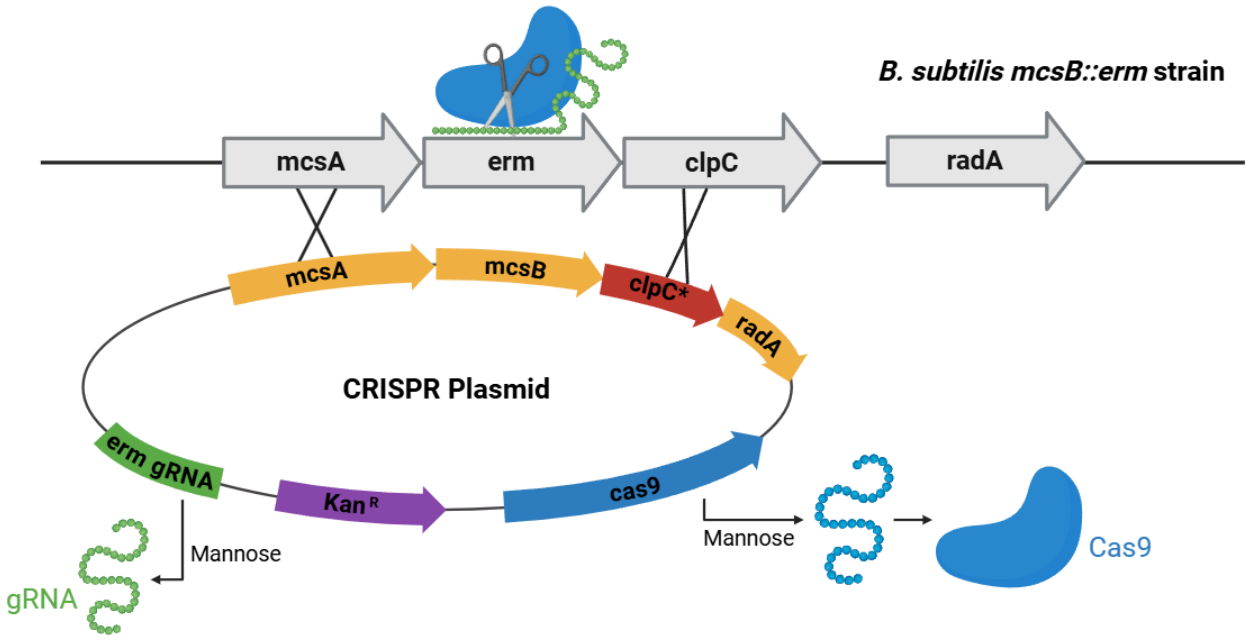

Figure 7. Modified CRISPR/Cas9 approach for creating mutations in native *B. subtilis clpC* gene. Image made in BioRender by K. Panchal.

The idea behind swapping residues to alanine (A) was to assess the specificity of residues to support the $ClpC^{MD}$-MdfA interaction. Alanine is a sterically small, neutral residue and therefore more chemically inert compared to the native charged residues; if a positive interaction between $ClpC^{MD}$-MdfA is unable to be formed as a result of swapping to alanine, then I would be able to determine that the native residue is necessary for interaction. Due to alanine being more neutral and the potential that for any given mutation made to the E190/K427/R443 group there would still be 2 charged residues that could potentially still support interaction, I decided to additionally pursue more aggressive side chain swaps. For this, I replaced positively charged residues, arginine (R) and lysine (K), with negatively charged residues (E) and vice versa, with the goal of inducing a negative interaction between $ClpC^{MD}$ and MdfA.

3.2 Only *mdfA*^{E190} mutants are able to disrupt the MdfA□ClpCP mediated negative feedback loop and cause high σ^F activity during sporulation

A key phenotype in *Bacillus subtilis* strains that have broken ClpC-MdfA interactions is high σ^F-related activity during sporulation. Previously, it has been shown by Camp Lab members that strains of *B. subtilis* lacking *mdfA* have increased σ^F activity and this phenotype can be replicated in strains that contain mutant ClpC N-Domain residues (data not shown). This is due to MdfA and ClpC working together during sporulation to progress the cell to metabolic shutdown by indirectly and directly contributing to a negative feedback loop that reduces σ^F in the forespore.

σ^F is responsible for activation of several genes within the forespore, including *clpC* and *mdfA*. When the MdfA-ClpCP complex forms, it degrades metabolic precursor molecules, slowing metabolism (consequently slowing gene activity including that of σ^F), and it degrades σ^F, creating a negative feedback loop. When MdfA and ClpC are unable to interact, σ^F and other metabolic precursors are stabilized and so σ^F-related activity skyrockets.

Our goal with this set of assays was to be able to measure the σ^F-related gene expression within the developing forespore and determine what role the $ClpC^{MD}$-MdfA interaction plays in the progression of metabolic shutdown. To do this, we created strains harboring a *lacZ* reporter gene under a *spoIIQ* promoter that could be used to confer how much σ^F-related activity was occurring. We expected that strains harboring mutations that break the $ClpC^{MD}$-MdfA interaction report a higher level of σ^F-related gene expression, and could indicate that the M-Domain is needed for the *in vivo* function of MdfA.

Cells were induced to sporulate, samples were collected every hour, then β-galactosidase activity was measured using a kinetic enzyme assay. β-galactosidase levels above background (WT *B. subtilis*, PY79, with no *lacZ* reporter gene) indicated σ^F-related gene expression and activity. The *lacZ* reporter gene consists of *lacZ* linked to a *spoIIQ* promoter, which is σ^F dependent. In otherwise wild type *B. subtilis* (See strain list for more details), σ^F-related activity starts low during the start of sporulation before picking up towards the middle of sporulation then slowing decreasing in the end (Figure 8A). Conversely, the removal of *clpC* causes lower and delayed σ^F-related activity. This is due to the pleiotropic effects associated with strains harboring Δ*clpC* (Figure 8A).

In strains harboring Δ*mdfA*, or ones that have residue swaps that break the ClpC N-Domain interaction to MdfA ($clpC^{Q11P}$, data not shown), σ^F-related activity is notably higher

during the later hours of sporulation (Figure 8A). The cause for the increased σ^F-related gene expression in these strains is due to MdfA being unable to perform its *in vivo* function that encourages formation of the active ClpCP complex, which is responsible for destabilizing σ^F and the degradation of metabolic enzymes in the developing spore.

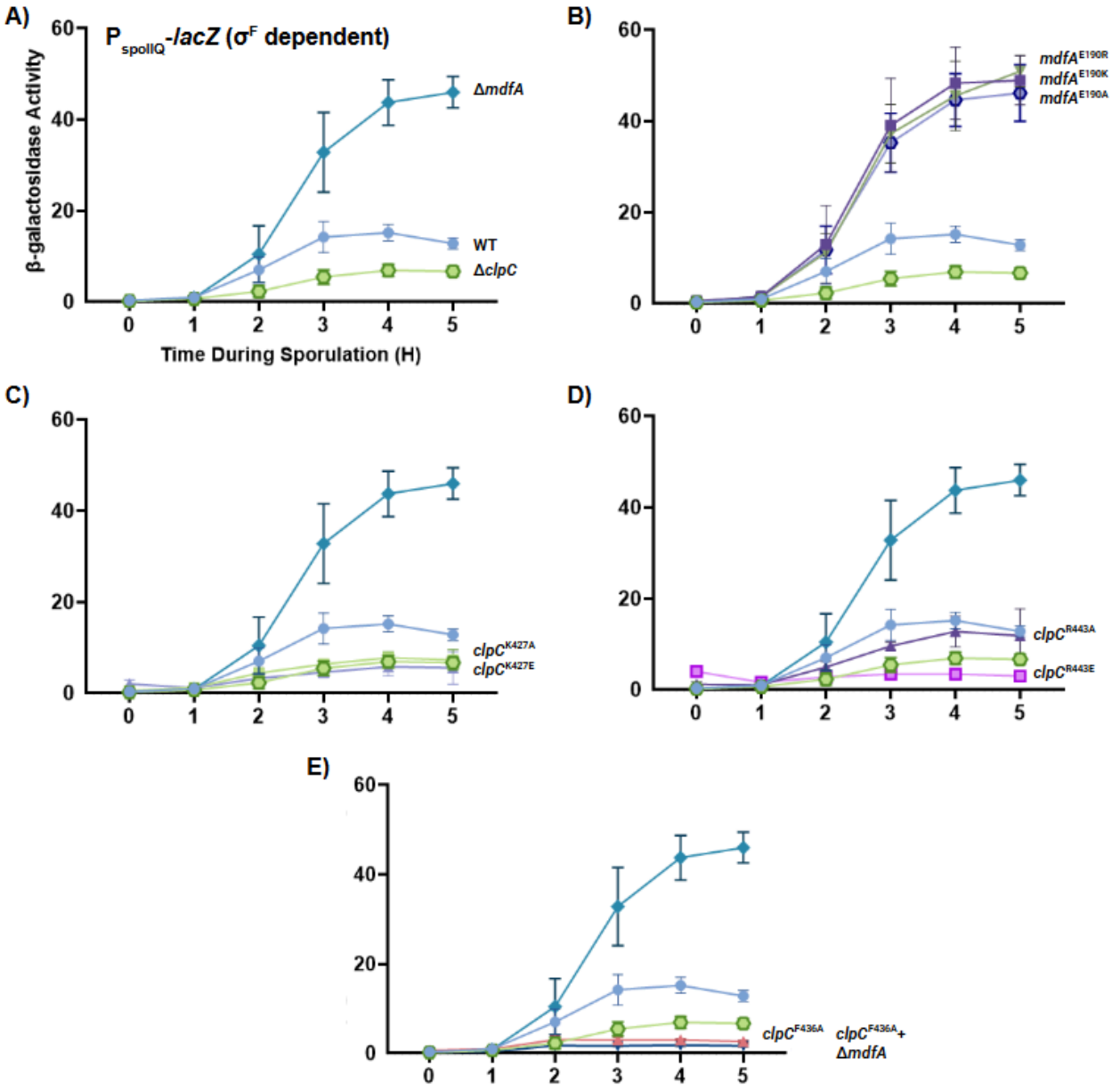

Figure 8. The *mdfA*$^{E190R/K/A}$ allele, similar to Δ*mdfA*, stimulates σ^F activity during sporulation; in contrast, the *clpC*$^{K427A/E}$, *clpC*$^{R443A/E}$ and *clpC*^{F436A} alleles did not appear to stimulate σ^F-related gene expression during sporulation. β-galactosidase production from σ^F-dependent P_{spoIIQ}-*lacZ* reporter was monitored during sporulation of otherwise wild

type cells (light blue circle, AHB881), Δ*mdfA* (teal diamond, SMB189), Δ*clpC* (green hexagon with border, CFB302), *mdfA*^{E190R} (purple square), *mdfA*^{E190K} (green flipped triangle), *mdfA*^{E190A} (blue hexagon with border), *clpC*^{R443A} (purple triangle), *clpC*^{K427A} (light green square), *clpC*^{R443E} (magenta square with border), *clpC*^{K427E} (light purple triangle), *clpC*^{F436A} (hot pink triangles), or cells containing *clpC*^{F436A}+Δ*mdfA* (dark blue triangles) (strains AHB881, SMB189, CFB302, JBB27, JBB30, JBB33, JBB56, JBB58, JBB62, JBB60, JBB14, JBB38 respectively). Control strains are shown for comparison and do not change between figures. Error bars indicate ± standard deviations based on at least n=3 replicates.

Beginning with the results collected on the MdfA variants, mutations to the *mdfA* E190 codon to either a positively charged residue (R/K) or a neutrally charged residue (A) resulted in higher levels of σ^F activity as sporulation progressed (Figure 8B). This was a shared phenotype with strains lacking *mdfA* (Figure 8A). Interestingly, strains with *mdfA*$^{E190A/K/R}$ tended to have slightly higher levels of measured activity compared to strains lacking *mdfA* outright. Overall, strains with variant MdfA had σ^F activity approximately 3x greater than otherwise WT strain activity around the later hours of sporulation.

With this initial result demonstrating that changes to E190 on *mdfA* could produce a heightened σ^F-related activity phenotype, we proceeded to make E190 complementary variants on the ClpC M-Domain. Residues K427 and R443 (results shown in Figure 8C and 8D respectively), identified as potentially interacting with E190 on MdfA, on *clpC*^{MD} were either changed to a neutral residue (A) or a negatively charged residue (E).

Starting with the K427 results, *clpC*^{K427A} and *clpC*^{K427E} had σ^F activity comparable to cells harboring Δ*clpC* with the cells harboring *clpC*^{K427A} having slightly higher activity and cells with *clpC*^{K427E} having slightly lower activity flanking Δ*clpC* (Figure 8C). In our R443 results, *clpC*^{R443A} and *clpC*^{R443E} had noticeably different results between each other (Figure 8D). *clpC*^{R443A} shared σ^F activity most similar to WT, but lowered and also appearing to have a delayed

σ^F-related activity pick up (Figure 8D). Conversely, *clpC*^{R443E} had activity comparable to *clpC*^{F436A}, with a peak in activity around hour 0 before sharply decreasing for the rest of sporulation. This is a pattern that was consistent during trials including *clpC*^{R443E} but had not appeared in strains previously.

Results including *clpC*^{F436A} were separated from other *clpC* mutations due to strains' exceptionally low σ^F activity. Cells harboring just *clpC*^{F436A} had no significant increase in σ^F activity during the entirety of sporulation (Figure 8E). These phenotypes were interesting to us, as the *clpC* mutants were able to grow vegetatively fine and did not appear to have the same slow growth phenotypes that cells harboring Δ*clpC* had (data not shown).

3.2.1 ClpC M-Domain variants do not become hyperactive in a MdfA-dependent manner

Given that all ClpC M-Domain variants had the opposite phenotype we expected, we tried to understand this unexpected phenotype by combining a *clpC* M-Domain mutation with a *mdfA* knockout. The thought behind this approach is that perhaps the *mdfA* knockout would "overpower" the low σ^F activity phenotype that's characteristic of all of our *clpC* mutants. We determined that including this additional *mdfA* knockout would be most beneficial for understanding the phenotype of cells harboring *clpC*^{F436A}, since they had the lowest σ^F activity by far (See Discussion for reasoning).

To conduct this experiment, we started with a strain that contained the P_{spoIIQ}-*lacZ* reporter gene at *amyE* and *clpC*^{F436A} at the native *clpC* locus (strain JBB14) and transformed in isolated chDNA that contained Δ*mdfA* to create a *clpC*^{F436A}+Δ*mdfA* strain (strain JBB38). If ClpC was hyperactive but MdfA-dependent, then removing *mdfA* would theoretically result in σ^F activity in the forespore increasing as ClpC would be unable to perform its role in metabolic shutdown without MdfA; however, when *mdfA* is additionally knocked out, σ^F activity did not

increase (Figure 8E). Instead, σ^F activity further decreased in cells harboring *clpC*^{F436A} when *mdfA* was removed.

3.3 *clpC*^{MD} mutants have a 10-fold decrease in sporulation efficiency

The results from the ClpC M-Domain mutants brought further questions on strains' ability to form spores and engage in the stages of sporulation successfully. Because the β-galactosidase assay requires cells to be able to form spores in order to measure ClpC-MdfA interaction, decreased ability to form spores could impact measurements. By measuring the amount of heat resistant spores a strain was able to form, we expected to assess why ClpC M-Domain variants had such low σ^F-related activity. To do this, a spore count assay was conducted to measure viable spores by colony forming units (CFU) (Figure 9).

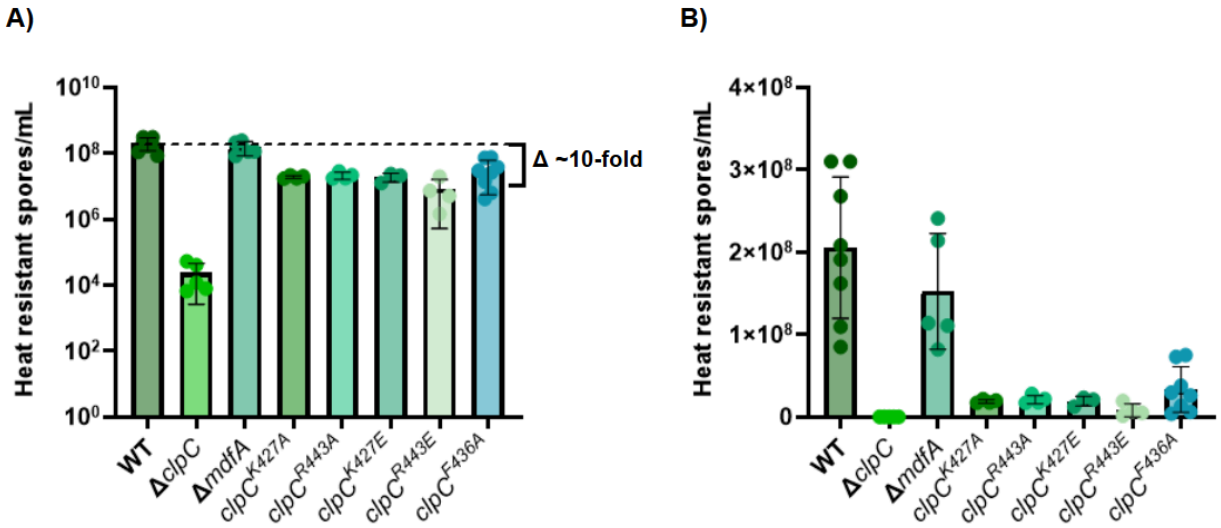

Figure 9. Cells with ClpC M-Domain mutants show 10-fold decrease in counts of heat resistant spores when compared to wild type and Δ*mdfA* containing cells (strains PY79 and SMB251 respectively), but do not have the same severe sporulation defect as cells with Δ*clpC*. WT, Δ*clpC*, Δ*mdfA*, *clpC*^{K427A}, *clpC*^{R443A}, *clpC*^{K427E}, *clpC*^{R443E}, *clpC*^{F436A} cells (strains PY79, CFB270, SMB251, JBB40/41, JBB42/23, JBB44/45, JBB46/47, SOB7 respectively) were induced to sporulate for 24 hours and the number of heat resistant

spores per mL was determined. Individual data points are shown (at least n=3) and bars indicate standard deviation away from mean spore efficiency for each strain. Biologically identical duplicates were run twice for *clpC*^{K427A}, *clpC*^{K427E}, *clpC*^{R443A}, *clpC*^{R443E} for a total of n=4 trials; *clpC*^{K427E} had 1 trial not included due to failure for any colonies to develop unexpectedly. A) Log scale view of spore counts. B) Linear scale view of spore counts.

Wild type and Δ*mdfA B. subtilis* strains are able to produce heat resistant spore counts around $2x10^8$ spores/mL. On the contrary, Δ*clpC* has a 10,000-fold reduction in spore counts with higher variability in CFU. Cells containing *clpC*$^{K427A/E}$, *clpC*$^{R443A/E}$, or *clpC*^{F436A} displayed a 10-fold reduction in heat resistant spore counts (down to 10^7 spores/mL) with significant variability between 10 to a 100-fold differences for R443E and F436A. Indeed, it appears that there is a decrease in sporulation efficiency for *clpC*^{MD} mutants. This indicated the need for an assay that could measure ClpC-MdfA interactions without the need for cells to form competent spores or engage with sporulation at all.

3.4 ClpC M-Domain and MdfA variants are able to protect against MdfA-toxicity during vegetative growth

Currently it is understood that *in vivo*, MdfA is only expressed during sporulation and within the forespore, and acts as an adaptor protein to ClpCP to induce metabolic dormancy in the developing spore. Previous Camp Lab members have shown that MdfA presence in the vegetative cell can cause cell toxicity due to interaction and subsequent activation of ClpCP (Massoni et al. 2025). To be able to understand the role of the ClpC^{MD} in facilitating the interaction between ClpC-MdfA, we chose to measure this phenotype. Additionally, given the challenges in interpreting the results from the ClpC mutants when measuring MdfA-ClpC

interactions that occur during sporulation, having a non-sporulation based assay would allow us to measure *in vivo* MdfA function without the cells needing to be able to form spores.

3.4.1 The IPTG-inducible MdfA toxicity test measures *in vivo* function outside of sporulation

An IPTG-dependent copy of *mdfA* was inserted into the *B. subtilis* chromosome to induce MdfA production in the vegetative cell. The presence of MdfA causes the oligomerization of ClpCP and inappropriate degradation within the vegetative cell, leading to toxicity and lysing (Figure 10). Cells can be rescued from MdfA-ClpC toxicity through mutations that break interaction or remove one of the interacting partners.

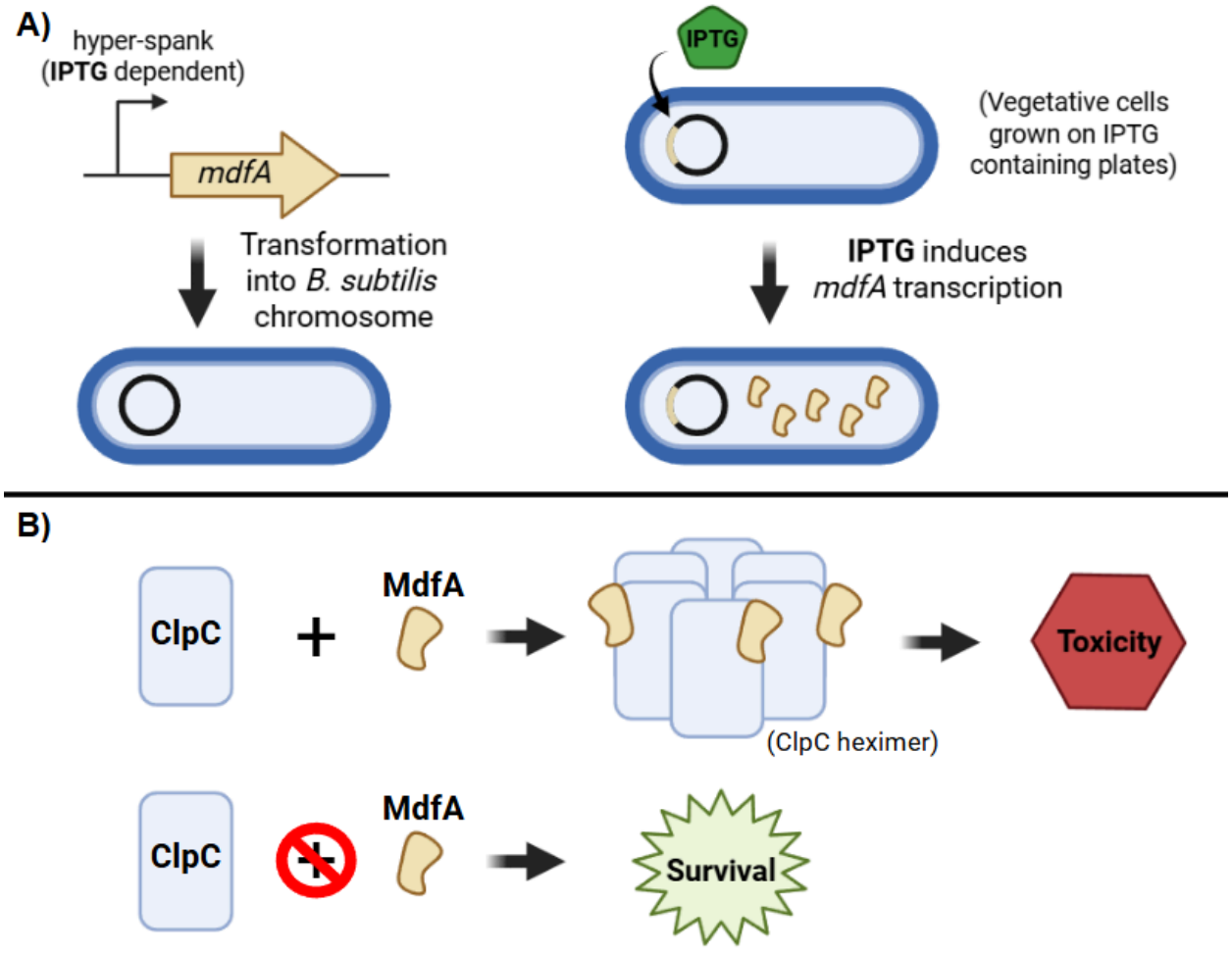

Figure 10. IPTG-inducible MdfA toxicity test. Figure made in BioRender.

All strains presented in these results, sans the true wild type, have this IPTG dependent promoter, but are referred to by their key mutation. Site-directed mutagenesis was performed on plasmids containing a copy of the *mdfA* gene to be inserted into the *B. subtilis* chromosome at *amyE*. IPTG at 1 mM is not inherently toxic to *B. subtilis*, unless strains harbor the additional IPTG-inducible *mdfA* gene (Figure 11A; Row 1). When strains are grown vegetatively on LB agar containing IPTG, the ClpCP-MdfA interaction induces toxicity (Figure 11A; Row 2). This phenotype of MdfA toxicity is ClpC dependent, as shown by the rescuing of cells from toxicity when *clpC* is knocked out (Figure 11A; Row 3).

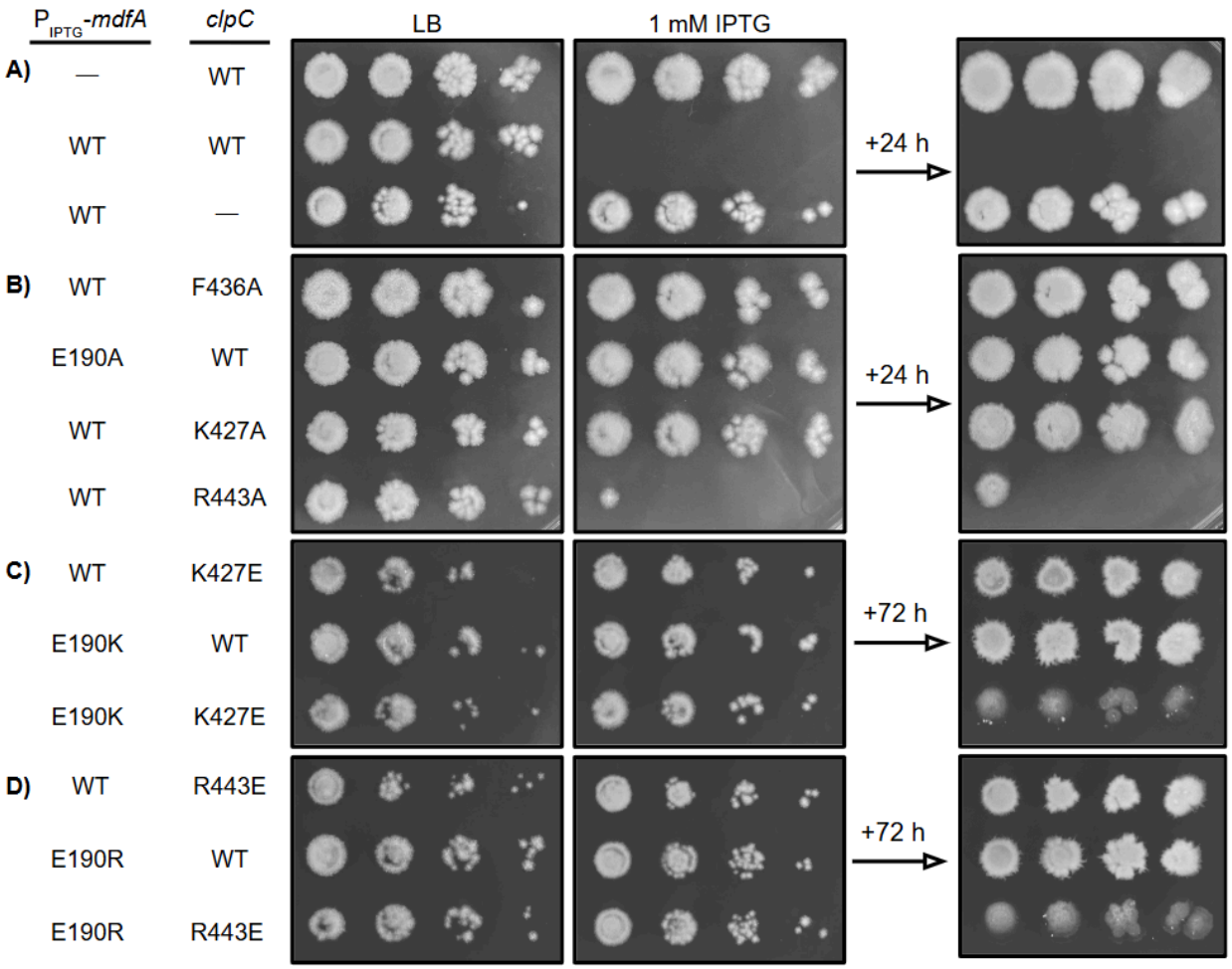

Figure 11. IPTG-related overexpression of *mdfA* in the vegetative cell causes cell death that can be persistently suppressed by single residue swap mutations and gene knockouts. Cell cultures are grown to approximately mid logarithmic phase and then plated in descending 10-fold dilutions on LB or LB + 1 mM IPTG plates. A) Strains without inducible *mdfA* gene (WT) or without *clpC* (Δ*clpC*) are protected from toxicity. Strains that harbor the inducible *mdfA* gene and have ClpC-MdfA interactions that are unbroken are not protected from toxicity (strains PY79, CFB241, and CFB189 respectively). B) Strains that harbor alanine mutations have mixed protection against toxicity. Strains harboring $clpC^{F436A}$, $clpC^{K426A}$, or P_{IPTG}-$mdfA^{E190A}$, fully protected against toxicity (strains JBB14, JBB48 and JBB25 respectively). Strains harboring $clpC^{R443A}$ lack protection against toxicity (strain JBB50). After 24 hours of additional development, strains kept their toxicity phenotypes. C) Single charge swap mutations on K427 or E190 have complete protection against toxicity, while double charge swap mutations have partial toxicity after 72 hours of additional development. Strains harboring $clpC^{K427E}$ or P_{IPTG}-$mdfA^{E190K}$ were able to grow on IPTG plates and kept their toxicity protection after further incubation (strains JBB52 & JBB23 respectively). Cells containing both $clpC^{K427E}$

and P_{IPTG}-*mdfA*^{E190K} suffered from toxicity after 72 hours (strain JBB68). D) Strains harboring *clpC*^{R443E} or P_{IPTG}-*mdfA*^{E190R} were able to grow on IPTG plates and retained toxicity protection after addition incubation (strains JBB54 and JBB21 respectively). Cells containing both *clpC*^{R443E} and P_{IPTG}-*mdfA*^{E190R} suffered from toxicity after 72 hours (strain JBB70). Images are representative of at least n=3 trials.

Through M-Domain charge swaps or complementary MdfA charge swaps, vegetative cells can be protected from toxicity. M-Domain K427 and R443 variants when swapped to the negatively charged residue (E) fully protected cells from toxicity (Figure 11C & 11D; Row 1); however, the neutrally charged residue (A) only protected cells harboring K427A (Figure 11B; Row 3). All P_{IPTG}-*mdfA*^{E190} mutations were sufficient to protect the vegetative cells from toxicity (Figure 11B, 11C, 11D; Row 2).

For certain mutants, the swap to a neutrally charged residue seemed to be able to break interactions between ClpC-MdfA better than others. For P_{IPTG}-*mdfA*^{E190A}, *clpC*^{F436A}, or *clpC*^{K427A} containing strains, cells were fully protected from toxicity (Figure 11B; Row 1). In contrast, *clpC*^{R443A} lacked protection from toxicity past the 10^{-2} colony dilution (Figure 11B; Row 4).

3.4.2 Double charge swap mutants show partial toxicity to cell during vegetative growth

With the results of our single charge swap mutants to *clpC* or *mdfA* showing a break in interaction and therefore protection from toxicity, we were curious to know if we could restore the toxic interaction by pairing charge swapped ClpC and MdfA together. To do so, a double charge swap mutant with negatively charged residue swapped into ClpC and positively charged residue swapped into MdfA was made. After the initial 48 hour incubation period, double charge swapped mutants protected against toxicity (Figure 11C & 11D; Row 3); however, when plates were allowed to develop for an additional 72 hours, double charge swap mutants showed signs of toxicity stress: colonies lightened in color and were noticeably less dense than adjacent strains.

This was in contrast to the single charge swap mutants that remained completely protected from MdfA related toxicity even after additional growth time. It was determined that the double charge swap mutants held a partial toxicity phenotype and a partial interaction between ClpC-MdfA when key residue charges were swapped.

CHAPTER 4:

DISCUSSION

4.1 Summary

Our goal as stated in the introduction was to determine if the ClpC M-Domain facilitates the *in vivo* function of MdfA during *Bacillus subtilis* sporulation. We were successful in making mutations in both the native *clpC* and *mdfA* gene and were able to see through the kinetic β-galactosidase assay that *mdfA*^{E190} mutants demonstrated a broken negative σ^F feedback loop; however, we ran into issues with our *clpC* M-Domain mutants when trying to prove this interaction from the ClpC side. We believe that the *clpC* M-Domain mutants have pleiotropic effects that are difficult to interpret through this assay; further analysis done on spore counts of the *clpC* mutants revealed a 10-fold spore defect.

To navigate this, we had to modify our hypothesis to accommodate the fact that our *clpC* M-Domain mutants could not be measured during sporulation. Our goal became to determine if the ClpC M-Domain facilitates the *in vivo* function of MdfA in *Bacillus subtilis*. To test this, we used an IPTG-inducible MdfA toxicity test, where cells would be safe from MdfA-mediated toxicity if ClpC and MdfA were unable to interact. We were able to demonstrate both from a MdfA-side and a ClpC-side that the M-Domain plays a key role in facilitating interaction. We demonstrated this both through single charge swap mutations to *mdfA*^{E190}, *clpC*^{K427}, *clpC*^{R443}, and *clpC*^{F436}, in addition to double charge swap mutations that partially restored interaction.

Through this paper we have sought to show that the ClpC M-Domain is a key partner in helping to facilitate the interaction between ClpC and the adaptor protein MdfA. We

accomplished this goal outside of sporulation for both ClpC and MdfA, but were only able to accomplish this goal during sporulation for MdfA. Nevertheless, we can say with confidence that the M-Domain is a specialized and important domain to ClpC, and we are moving towards understanding the role it plays in the interaction and function with MdfA during sporulation.

4.2 Discussion of selection of MdfA-specific ClpC M-Domain alleles

Our goal of locating residues on ClpC and MdfA that could be modified using mutagenesis for the purpose of assessing ClpC-MdfA interactions was successful. We were able to select a handful of alleles on *clpC* and one on *mdfA* that we then successfully mutated and confirmed using Sanger and Nanopore sequencing. We specifically selected residues that were predicted to either have strong hydrophobic attractions (F436) or strong electrostatic attractions (R443 & K427 on ClpC, E190 on MdfA). By doing this, we hoped to target key areas for interaction on the very limited interface that ClpC and MdfA share.

In the past, Camp Lab members have been able to do analogous work in proving that interactions occur between the ClpC N-Domain and MdfA by mutating select alleles that only affected the interaction between ClpC and MdfA (Massoni et al. 2025). However, because of the limited number of residues making up the M-Domain, we have not yet determined a ClpC M-Domain and MdfA *specific* residue. Granted with how small the M-Domain is–around 55 residues–it is possible that it does not have strict specificity to certain adaptor proteins, MdfA included.

It is worth noting that we made our decision for which residues to target based primarily on the AlphaFold predictions generated by collaborators in the Carroni Lab. To increase the chances of selecting important residues, we combed through previous literature that discussed

conserved residues on the ClpC M-Domain. There was a chance that, because there is a lack of physical evidence for how the ClpC M-Domain and MdfA are aligned in reality, that the residues we selected might not serve as true interaction points between ClpC and MdfA. However we believe our results support previous work that documents the accuracy of models produced by AlphaFold predictions (Evans et al. 2022).

4.2.1 The novel structure of MdfA could impact the way ClpC M-Domain was expected to interact with adaptor proteins

Initially when looking for residues on MdfA to selectively target, we hoped to see a stronger hydrophobic area that we could exploit. MecA, a frequently studied adaptor protein of ClpC, has a structure that includes a hydrophobic pocket that the ClpC M-Domain, specifically the F436 residue, can tuck into (Figure 12). This creates a hydrophobic stabilizing interaction; however, this was not the case for the structure of MdfA. Instead, MdfA has a helix that is predicted to be decorated with mostly negatively charged residues, with minimal hydrophobic areas in the areas we would expect the M-Domain to favorably interact with (Figure 13A & 13B).

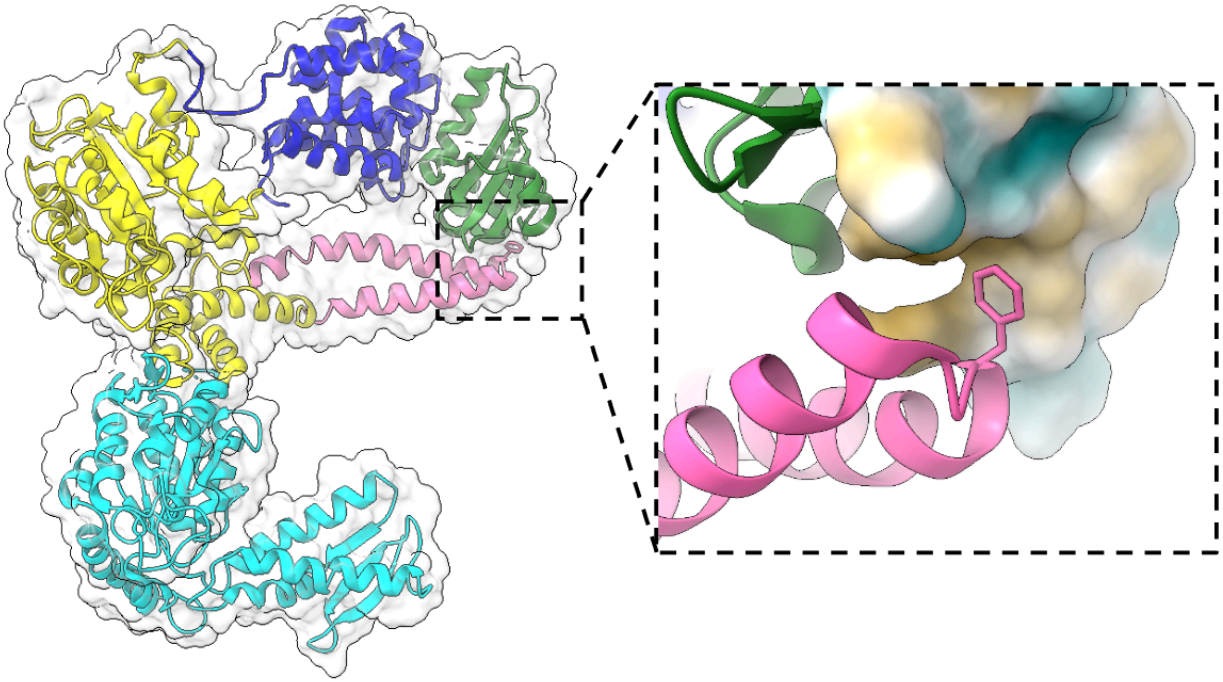

Figure 12. ClpC monomer heterodimer with MecA, ChimeraX visualization of PBD file 3J3T from Liu et al. (2013) cryo-EM experiments. Hydrophobic surfaces are mapped on MecA (dark green) in orange while hydrophilic surfaces are shown in blue. The F436 residue on the ClpC M-Domain fits into a hydrophobic pocket within MecA.

Looking deeper into predicted hydrophobic areas on ClpC and MdfA, it appears that the distant M-Domain helix harbors a collection of hydrophobic residues that create a hydrophobic "edge" to the M-Domain that is not equal on both helices of the M-Domain (Figure 13C & 13D). I suspect that this hydrophobic edge might serve as a site for adaptor proteins to come in and align properly with ClpC. It has been discussed previously by Annis et al. (2024) that the hydrophobic phenylalanine (F) located at the edge of the M-Domain is both strongly conserved and required in some species to form head-to-head interactions; additionally, the conserved charged residues, R443 being one such residue, help to support interactions by forming intramolecular salt bridges (Carroni et al. 2017).

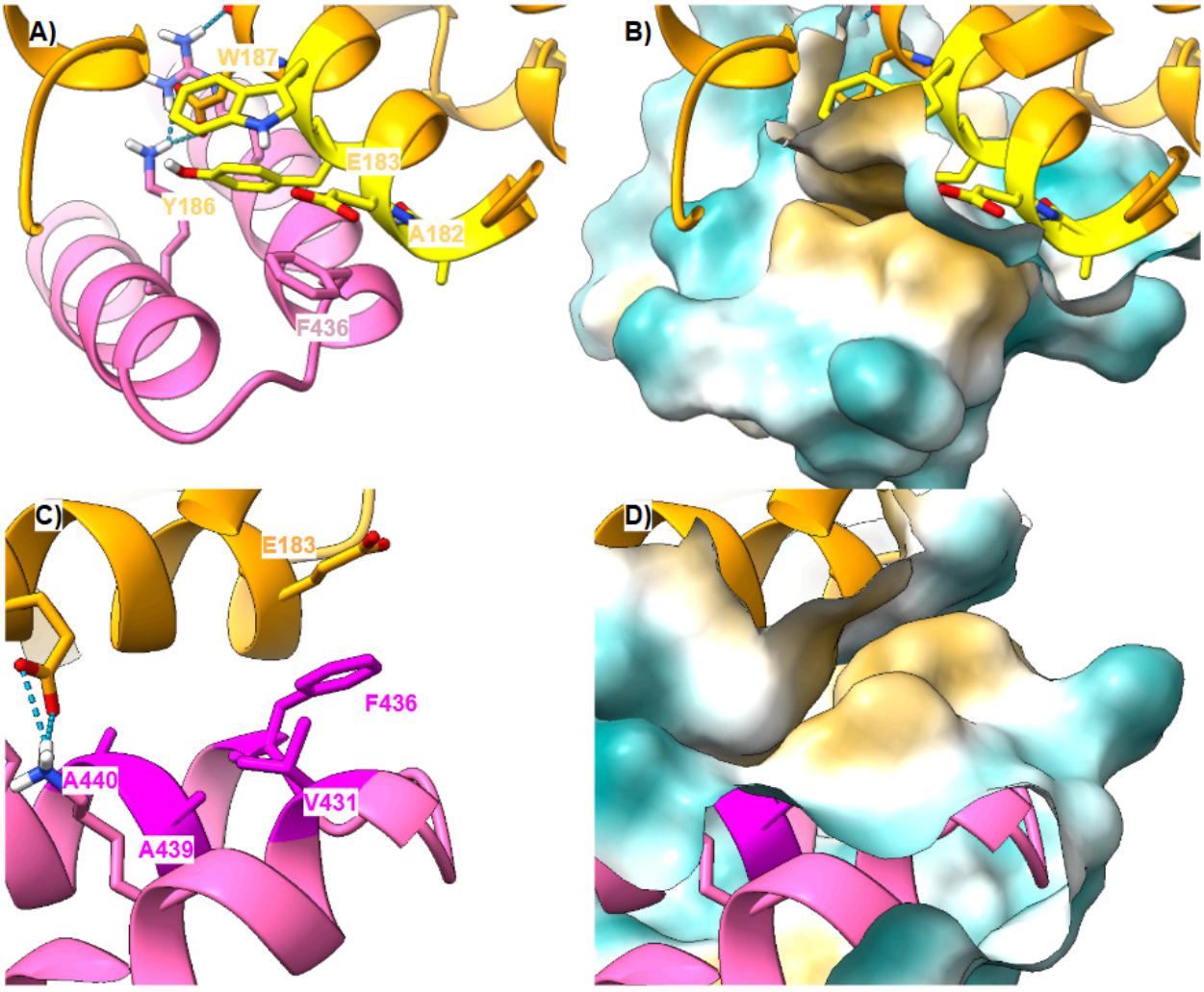

Figure 13. Mapped surface of predicted hydrophobic areas between ClpC M-Domain (hot pink) and MdfA (orange). A) Residues on MdfA that share proximity to ClpC F436 are shown in yellow. B) Overlaid hydrophobic surface map of MdfA residues. E183 on MdfA is aligned parallel with the F436 aromatic ring while Y186 on MdfA is predicted to angle down towards the closer helix of ClpC. C) Hydrophobic edge on the tip of the ClpC M-Domain. Residues suspected to contribute to this hydrophobic area are highlighted on ClpC in magenta. D) Hydrophobic edge on the tip of the ClpC M-Domain surface view. Hydrophobic preference is indicated by orange coloring while hydrophilic preference is indicated by blue coloring.

4.2.2 Discussion on how R443 and K427 mutations might impact the steric compatibility of ClpC and MdfA

On ClpC, R443 was interesting to me: Its positioning on the same helix and surface as F436 made me curious if it might ultimately affect the hydrophobic interactions the M-Domain uses to potentially interact with adaptor proteins or other M-Domains. In our experiment, we swap R443 with either a neutral alanine (A) or a negatively charged glutamic acid (E). The thought behind the swap to a negatively charged glutamic acid was to create a repulsive force between ClpC and MdfA. I do think that this goal was accomplished, especially looking at later results, but the swap to glutamic acid cannot be used to say that R443 is specifically required for the ClpC-MdfA interaction. Rather, since R443 exists on the same alpha helix as F436, it could be that some phenotypes, like the aggressive drop in σ^F-related activity, could be as a result of a repulsive interaction between $ClpC^{R443E}$ and $MdfA^{E190}$ that interferes with the interaction of F436 with areas on MdfA; essentially causing the R443E mutant to appear similarly to a F436A mutant. It could be that if we had swapped R443 with an aspartic acid (D), a slightly shorter negatively charged residue, that we would have been able to hone in more on the interactions that R443 helps create as opposed to skewing the role F436 plays in interactions.

One residue that I have not seen discussed previously around this topic of *B. subtilis* ClpC M-Domain interactions was K427. During my literature review, I found work done by Wang et al. (2011) that pointed to the importance of D428 for MecA-ClpC complexing, but nothing on K427 and what role it might play in the complexing of MdfA-ClpC during sporulation. Wang noted that D428A had little impact on formation of the ClpC hexamer, but reduced ATPase activity. I think it is reasonable to think that potentially K427A or K427E could do something similar in ClpC-MdfA. Our primary reason for selecting K427 for mutagenesis was because of ChimeraX predictions that placed K427 in an advantageous spot to

electrostatically interact with E190 on MdfA. Additionally, K427 exists on the M-Domain helix adjacent to R443 and F436, potentially limiting unintended steric or electrostatic clashes with other important residues caused by swapping to K427E.

In this paper, we have not confirmed that MdfA, when E190 is mutated, is still folding properly. To confirm this, we could have performed a western blot, but within the timeframe of this project, this would not have been achievable; however, we find our MdfA toxicity assay results suggest that MdfA, even with E190 mutations, is still functional as it is able to cause toxicity as seen by our double charge swap results (See Figure 11C & 11D, Row 4). It is also important to note that within this project there are two "types" of MdfA: one that is induced by IPTG in the vegetative cell, and one that is natively induced by σ^F during sporulation. It is worth noting the possibility that MdfA with any E190 mutation might not be as effective as the true wild type MdfA, as it is expressed in the forespore.

4.3 Assessing the β-galactosidase results

The β-galactosidase assay is a population based assay that we used as a proxy to measure σ^F-related gene expression during sporulation. Disruption of *in vivo* MdfA and ClpC function breaks the negative σ^F feedback loop, resulting in higher levels of σ^F-related gene expression in the developing spore. While we saw that our mutations to *mdfA*^{E190} had this indicative phenotype, all of our mutations to the *clpC* M-Domain had varying degrees of below wild type levels of σ^F activity. From this, we can say that, while the *mdfA* mutations support our hypothesis that interaction with the M-Domain is necessary for *in vivo* function of MdfA, we are not able to use our *clpC* mutation results to support this conclusion in the context of this assay.

In terms of why our *clpC*^{MD} mutants had surprisingly low σ^F activity, three potential possibilities for why this could be occurring came to mind: ClpC M-Domain variants lose their

ability to hold an inactive conformation and therefore become hyperactive in the forespore (either in an MdfA independent or dependent manner), or ClpC M-Domain variants cause wider pleiotropic effects during sporulation both in the mother and forespore cell. With this assay, we could rule out if the ClpC M-Domain variants caused ClpC to become hyperactive in a MdfA-dependent manner (See Results Figure 8E), but the other two possibilities are not distinguishable using this assay and procedure.

We believe that there is a chance M-Domain mutations cause ClpC to become hyperactive because of work done by Carroni et al. (2017) that showed through Cryo-EM imaging of *S. aureus* ClpC, mutations to the M-Domain caused loss of the inactive conformation. To summarize briefly, the ClpC M-Domain forms head-to-head interactions with other free ClpC monomers via M-Domain interactions, potentially serving as an inactive confirmation mechanism that ClpC is held in until environmental conditions are met (adaptor protein interaction, binding of substrate, etc.) that force ClpC into an active confirmation. It is not yet understood the molecular kinetics of this interaction, how relevant this is to ClpC in *B. subtilis*, or at what rate ClpC might be in this confirmation during sporulation, but it is theorized that this interaction can provide post-translation regulation of ClpC activity.

When we were considering if ClpC could be hyper active, we had the lingering question of whether or not a hyperactive ClpC was still MdfA dependent or not. If ClpC was hyperactive but MdfA-dependent, then it could be that the removal of *mdfA* would produce a phenotype similar to that of just an *mdfA* knockout, and σ^F activity would increase due to lack of ClpC-MdfA suppression. Instead, we saw that σ^F activity remained the same, or even slightly lower than with just the *clpC*^{F436A} mutation. This felt reasonable to conclude that ClpC, if hyperactive, does not remain MdfA dependent to degrade molecules in either compartment. It

could be instead that ClpC is MdfA-independent and that paired with non-forespore-specific pleiotropic effects cause lower than expected σ^F activity during sporulation as measured by the β-galactosidase assay.

4.4 Assessing the spore count results

The goal of the spore efficiency assay was to ensure that the mutations we made to the ClpC M-Domain would not affect the cells' ability to produce spores. With the assays used in this paper being based around the events of sporulation and our goal being to test *in vivo* functions of MdfA, it was important to us that the cells we were testing were still able to produce spores. Using this assay, we were able to identify where potentially some of our issues with the β-galactosidase assay were occurring. Indeed, we saw that *clpC*^{MD} mutants had, on average, a 10-fold decrease in heat resistant spore counts when compared to WT *B. subtilis*. This phenotype does not align with our overall hypothesis and goal to have *clpC*^{MD} mutants that do not have sporulation defects so that we could determine if the *in vivo* function of MdfA during sporulation requires interaction with the ClpC M-Domain.

The biggest potential source of error in the spore count protocol currently used is the duration of the incubation time potentially selecting against the mutations we made. Cells are cultured in starvation medium for 24 hours before being exposed to high temperatures to remove all cells unable to form spores. This long culture period forces the cells into a sporulation strategy, but if cells are unable to produce spores perhaps due to lack of ClpC functionality, they are being selected against. Even if we assume the mutation rate is constant between all strains, there is always going to be some amount of mutations that are picked up. For cells that have no issue sporulating, the majority of cells will remain similar to the original strain; however, for

cells that do have issues sporulating, there is a potential for a mutation to arise that outcompetes the original strain we are attempting to measure. With such a long incubation period, there is variability in when a mutation arises and outcompetes its progenitor strain, as well as what kind of mutation arises. For strains that lack *clpC*, a longer incubation period poses less risk of cells regaining *clpC*, which is why we see consistently low spore counts.

This potential skewed selection force is a possible reason for why we occasionally see dramatic fluctuations between data points of $clpC^{MD}$ mutants. Notably, $clpC^{F436A}$ and $clpC^{R443E}$ had approximately a 10-fold fluctuation. The other $clpC^{MD}$ mutants ($clpC^{K427A}$, $clpC^{K427E}$, $clpC^{R443A}$) did not have as great of variability. Whether that was luck or a true reflection of the spore producing ability of these strains is unclear. Each strain had at least 3 trials but reflecting on this, it seems better to increase the number of trials. Additionally, not all strains might be able to successfully navigate the stationary phase, especially if the strain already struggles with producing spores or handling stress.

For improving our methods of the spore count assay, we are considering adopting a procedure similar to the induction of sporulation via resuspension method we use to collect time point samples for the β-galactosidase assay. We would culture our cells for around 3 hours at ideal temperatures in a nutrient sufficient media, then spin and resuspend cells in a nutrient deficient media to induce sporulation. Allowing our cells to sporulate for a given amount of time before killing any cells unable to sporulate in a heat bath and proceeding to dilute and plate cells as described in the original procedure.

4.5 Connecting the β-galactosidase and spore efficiency results

After seeing our *clpC*^{MD} mutants had the opposite phenotype we expected, we tried to determine if the issue was caused by lower spore formation ability. Ultimately, we saw that overall all *clpC*^{MD} mutants had around a 10-fold decrease in spore formation ability. Taken together, the β-galactosidase and spore count assay have the same trend, but do not align in magnitude the same way. It is interesting how a strain that lacks *clpC* outright, despite having a 10,000-fold difference in spore count, has higher gene activity than some of our *clpC*^{MD} mutant strains. The number of spores a strain is able to produce does not seem to accurately represent the gene activity a strain has during sporulation.

It is important to discuss how the combination of reduced spore formation and the population-based approach might have impacted our results. As mentioned previously, the β-galactosidase assay is a population-based method, where the average enzyme activity detected is factored against the number of cells the sample contains (Massoni et al. 2025). Our *clpC*^{MD} mutants have WT levels of cell densities during sporulation, but from our spore count assessment we know that only 1:10 cells are able to produce spores. It could be that our *clpC*^{MD} mutants do in fact disrupt the negative feedback loop and cause higher σ^F activity in the developing spore, but because 90% of cells in the population cannot form spores, the average σ^F activity reads low.

If ClpC was hyperactive as a result of loss of its inactive conformation, it might not necessarily negatively affect the function ClpC provides in the forespore. In other words, it could be that the negative σ^F feedback loop that ClpC contributes to is actually strengthened as a result of our mutations. Currently, we believe that MdfA's *in vivo* function is to complex with ClpC and cause the targeted degradation of metabolic enzymes as well as σ^F that eventually lead to the progression of dormancy (Riley et al. 2024). With that in mind, if ClpC is over active in the

forespore, it could be that ClpC still is able to fulfill its degradation role within the forespore, with or without MdfA.

Potentially, the more pressing issue is the pleiotropic damages and loss of function that occur in the mother cell. The mother cell is responsible not only for providing itself with the necessary metabolic precursors that go on to build macromolecules needed for TCA, amino acid synthesis, translation, but it also provides the same precursors to the forespore via the feeding tube. ClpC is expressed both in the mother and spore cell, but while an overactive ClpC might not change much for the forespore, it could negatively impact the mother cell's ability to provide metabolic precursors for itself and the forespore. It could also be that the entry into sporulation is delayed or reduced completely. Either or both options could explain the drop in the number of cells that are able to produce spores.

4.6 Assessing the IPTG-inducible MdfA toxicity assay results

Our hope with this experiment was to find a work-around for ClpC M-Domain mutants that were unable to enter sporulation, which we were able to do. It is worth noting how MdfA is an adaptor protein that is only expressed in the forespore during sporulation, and its *in vivo* function is therefore exclusive to the events of sporulation. Our hypothesis as stated in the introduction was to determine if the ClpC M-Domain was required for the *in vivo* function of MdfA during sporulation. The IPTG-inducible MdfA toxicity assay does not occur during the events of sporulation; however, it demonstrates the general function of MdfA and ClpC: to cause degradation when complexed together. We were able to show that most single allele swaps made to the *clpC* M-Domain or MdfA were able to prevent toxicity; additionally, we were able to show that our double allele swaps were able to partially restore interaction. Indeed, we are not yet able

to definitively say that the ClpC M-Domain is required for *in vivo* function of MdfA during sporulation, but our results from this assay confidently demonstrate the M-Domain as an important interaction point between ClpC and MdfA.

As mentioned, all but one single charge swap mutants were able to break the interaction between ClpC and MdfA, that mutant being *clpC*^{R443A}. Considering the R443A mutation also did not fully interrupt the negative feedback loop and had σ^F activity most similar to WT in the β-galactosidase assay, this was not surprising. We think this could demonstrate that the R443 residue might not be specific to the MdfA interaction, despite its documented importance for other M-Domain functions (Carroni et al. 2017). This is further supported by the fact that R443 had 1 predicted hydrogen bond interaction to the E190 residue on MdfA where K427 had 2 predicted interactions. Additionally, this might indicate that results we have for R443E might be as a result of electrostatic repulsion and potentially interfering with the K427 residue's role in facilitating interaction.

From our results, we believe that the ClpC K427 residue is important for the MdfA interaction. We found it indicative that the K427A mutation was enough to protect against toxicity. From our literature review we could not find documentation on if K427 was an important contact point for other adaptor proteins. We did, however, find work discussing how D428 could be altered with little impact on the ability of ClpC to oligomerize with MecA (Wang et al. 2011). It could be that while residues like F436 on the M-Domain are important for any adaptor protein interaction, K427 serves as a more specific point of contact for MdfA-ClpC interaction.

As for why our double charge swap mutants, cells harboring either *clpC*^{K427E} and P_{IPTG}-*mdfA*^{E190K} or *clpC*^{R443E} and P_{IPTG}-*mdfA*^{E190R}, had partial toxicity phenotypes: we believe that

they restore interaction, but might be slightly misfolded. Since MdfA is much smaller in size than ClpC, it is very possible that a charge swap to E190 causes MdfA to be harder for ClpC to bind and recognize and vice versa. It is possible that with the charge swaps, ClpC and MdfA recognize each other less often than they otherwise would if we had not mutated them. Despite this, we can tell that charge swapped ClpC and MdfA can still recognize and bind with one another in some capacity since, after the additional incubation, cell cultures begin to lyse. It could be that it takes longer for MdfA-ClpCP mediated degradation to happen and cells can increase the rate of protein synthesis to compensate initially when there is an abundance of nutrients, but eventually the toxicity becomes evident.

In the future, a better overall experimental design for the IPTG-induced MdfA toxicity assay might include controlling for differences in culture densities. In the current procedure, cultures are grown for 6 hours at 37ºC, to when cells should be at mid-logarithmic phase (OD_{600} ~0.5), but I did not adjust the cell densities between strains. Originally, the procedure called for growing cultures at room temperature for a longer amount of time, the adjustment to cell densities served to correct for the differences in growth between strains lacking *clpC* that cause a slow growth phenotype; however, through troubleshooting and experimentation, I determined that by growing all strains for a shorter amount of time at 37ºC, a similar effect could be achieved. I do not believe that the decision to not correct for cell densities played a major role in the results generated.

4.7 Connecting *in vivo B. subtilis* toxicity assay results with *E. coli* B2H assay results

The work done in *B. subtilis* presented in this paper was part of a collaborative effort with fellow Camp Lab researcher, Jade Morrison, who conducted complementary work in *E. coli* to

create a fuller picture of how the M-Domain facilitates the ClpC and MdfA interaction. The goal with both of our projects was to create mutants that affected interaction on the ClpC^{MD}-MdfA interface and measure resulting interaction levels between ClpC and MdfA. Morrison's work approached this goal from within *E. coli*, measuring protein-protein interactions using a Bacterial 2-Hybrid (B2H) assay; my work approached this goal from within *B. subtilis*, originally hoping to quantitatively measure interactions during sporulation with the β-galactosidase assay but eventually switching to qualitatively measuring interactions outside of sporulation with the MdfA toxicity assay. When our work is taken together, we see consistencies in the level of interaction measured for the matching mutants we made for our respective assays. Supporting our respective hypotheses about the M-Domain's role in supporting interaction between ClpC and MdfA.

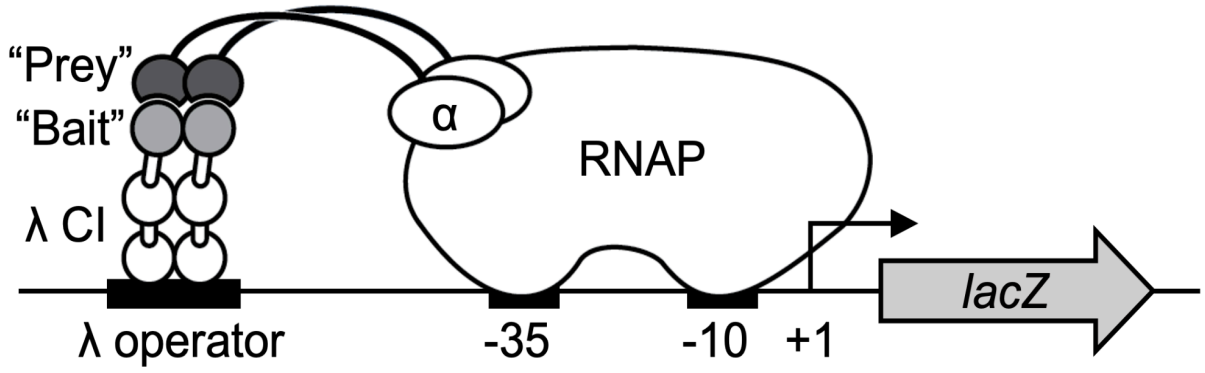

Figure 14. Bacterial 2-Hybrid (B2H) assay setup, figure from Dove and Hochschild (2004). A weak RNA polymerase (RNAP) is linked to a MdfA "prey" molecule. Upstream, a ClpC monomer "bait" is linked to a λ operator. Interaction between the bait and prey molecules allows for RNAP to bind and transcribe *lacZ* gene.

As discussed previously, outside of control strains, only *mdfA*^{E190} mutants could be interpreted successfully using the β-galactosidase assay in *B. subtilis*, while all *clpC* M-Domain mutants had phenotypes that were unable to be interpreted. For those *mdfA*^{E190} mutants, however,

when comparing B2H and β-galactosidase assay results, we saw phenotypes that indicated that the interaction between ClpC and MdfA had been broken. In the B2H assay, *mdfA*^{E190} mutants had low levels of interaction and in the β-galactosidase assay they had high σ^F activity during sporulation. Furthermore, cells harboring *mdfA*^{E190} mutations are no longer toxic in the MdfA toxicity assay. These results suggest that E190 is a residue that is necessary for the interaction between MdfA and ClpC.

The drawback of both the B2H assay and the MdfA toxicity assay is that the interactions between ClpC and MdfA do not occur during sporulation. The B2H assay occurs in *E. coli*, and measures interaction between a ClpC monomer and MdfA, both attached to their respective components that allow for the measuring of interaction related gene expression (Figure 14). This setup does not allow for ClpC to assemble into its native heximer form. The MdfA toxicity assay does take place in *B. subtilis*, but in the vegetative cell, which is a genetically–and chemically–different state than the developing spore. However, these drawbacks are also a strength to the assays we chose to pursue. Without the MdfA toxicity assay, we would have limited ways to assess ClpC-MdfA interactions in *B. subtilis*.

Table 5. Summary of mutant phenotypes measured in *E. coli* Bacterial 2-Hybrid (B2H) assay, or β-galactosidase and MdfA-toxicity assays conducted in *B. subtilis*.

		B. subt β-galactosidase Assay	*B. subt* MdfA-Toxicity Assay	*E.coli* B2H Assay
mdfA	*clpC*	Interaction?		
E190A	WT	no	no	no
E190K	WT	no	no	no
E190R	WT	no	no	no
WT	F436A	*	no	no

WT	K427A	*	no	partial
WT	R443A	**	yes	yes
WT	K427E	*	no	no
WT	R443E	*	no	no
E190K	K427E	—	partial	partial
E190R	R443E	—	partial	partial

*data not interpretable by this assay
**$clpC^{R443A}$ has activity similar to WT

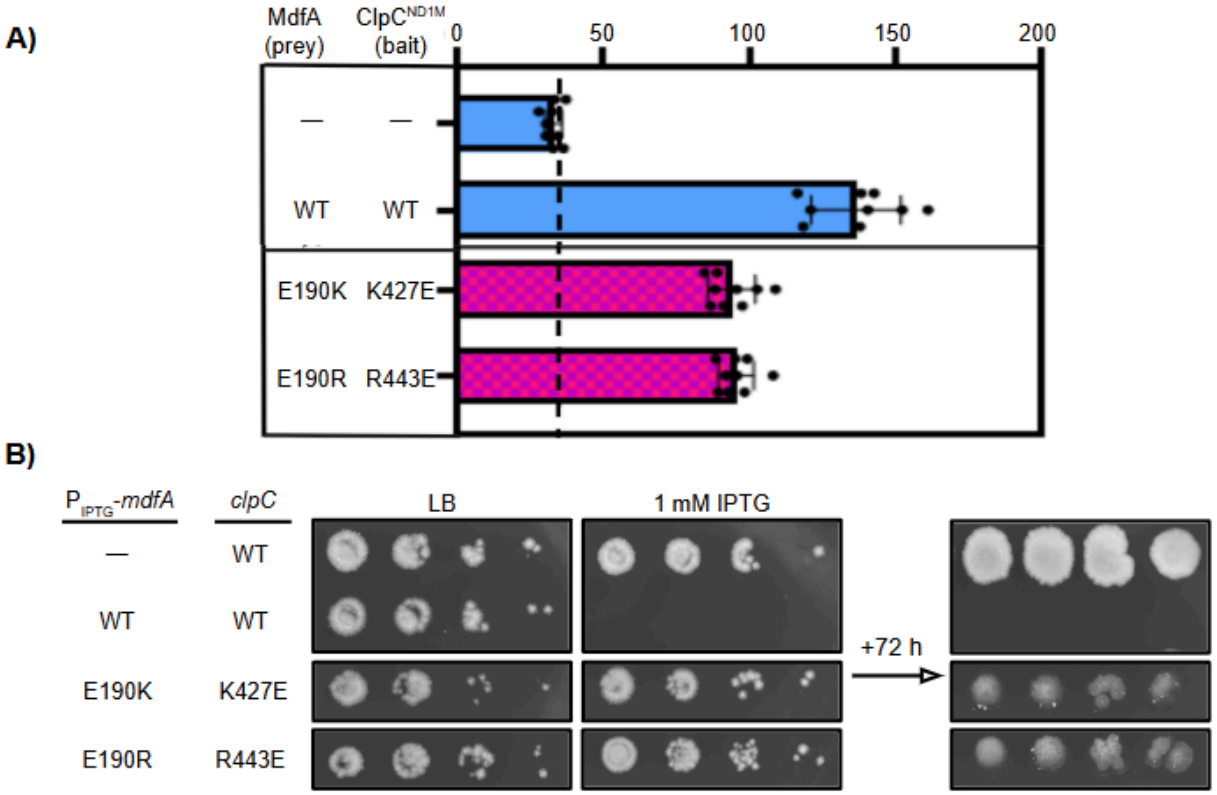

Figure 15. Example comparison of data collected in *E. coli* B2H assay done by Jade Morrison (A) to IPTG-inducible MdfA toxicity assay done by Jen Butler (B). A) *B. subtilis* ClpC^{ND1M} bait protein is expressed on the surface of *E. coli* RNA polymerase and interaction with complementary *B. subtilis* MdfA prey protein causes expression of *lacZ*. Higher levels of enzyme activity indicate higher interaction between bait and prey protein. B) MdfA expression in vegetative cells can be curbed by breaking the interaction between ClpC-MdfA. Growth on 1 mM IPTG-containing plates indicate a broken interaction between ClpC and MdfA while full or partial interaction indicates toxicity. The first row of each figure represents the negative control for each assay, the second row represents the positive control. Double charge swap mutant ClpC-MdfA show partial interaction phenotypes for both assays.

Between the B2H assay results and the IPTG-inducible MdfA toxicity assay results, our data overlaps well. We were able to see and measure phenotypes that indicate broken interaction between ClpC and MdfA for all of our shared mutants, excluding *clpC*^{K427A} (Table 5). Most excitingly, we both saw partial interaction for the double charge swapped mutants that aimed to restore interaction (Figure 15).

In my results, K427A was sufficient to break the interaction between ClpC and MdfA, and fully protected with no toxicity evolving even after additional incubation time. In the B2H assay, however, the K427A mutation only partially reduced the interaction between ClpC and MdfA. It could be that the cells harboring *clpC*^{K427A} are still partially interacting with MdfA and incurring some toxicity, but are able to appear fully protected from the toxic interaction since that interaction is only partial. It is much harder to distinguish between partial and broken interactions using the IPTG-inducible MdfA toxicity assay compared to the more quantitative B2H assay.

4.8 Future Directions

The biggest issue left with this project is figuring out how to deal with the pleiotropic effects caused by ClpC mutations during sporulation. As discussed, cells harboring $ClpC^{MD}$ variants have phenotypes that are hard to interpret in the β-galactosidase assay, we concluded that the most likely reason for this is due to the greater role of ClpC in the mother cell is being affected by our mutations. Specifically, ClpC helps regulate early entry into sporulation through its degradation of σ^H in the mother cell, allowing for the cascade of σ factors present during sporulation to begin (Nanamiya et al. 1998). There are two main ways we can shift our approach to get around these effects: perform assays that look at individual cells during sporulation or use two copies of *clpC*.

4.8.1 Individual cell microscopy based assays

As discussed, all of our cells harboring $ClpC^{MD}$ variants produced about 90% less heat resistant spores than wild type *B. subtilis*. When measuring σ^F related activity in the spore in a population based assay, we saw dramatic and unexpected drops in activity, potentially due to averaging activity by optical density. Instead, we propose using a microscopy based approach to search for individual cells that are able to form spores successfully and then observing fluorescent tagged proteins that ClpCP degrades during sporulation. To be brief, it has been demonstrated through fluorescent tagging experiments that ClpCP targets proteins such as CitZ in the forespore with bias (Riley et al. 2021; Riley et al. 2025). If mutations made to the M-Domain break interaction between ClpC and MdfA, then during sporulation the amount of GFP tagged CitZ should not decrease significantly.

In addition to this, we could insert a *gfp* gene (**G**reen **F**luorescent **P**rotein) that is dependent on σ^F related activity in the spore into cells harboring $ClpC^{MD}$ variants and then observe individual cells through fluorescent microscopy. Furthermore, this could help us to

distinguish if mutations to the ClpC M-Domain cause ClpC to become hyperactive or if there is just a strong pleiotropic effect associated with these mutations. Either method would help prove to us that some of the cells are still able to undergo spore formation, as well as if the M-Domain facilitates the *in vivo* role between ClpC and MdfA.

4.8.2 A secondary copy of clpC gene could reduce pleiotropic effects

The mother and forespore cell utilize the genetic information within their identical chromosome differently during sporulation. The *clpC* gene is used for different purposes between the two compartments and is expressed under different sigma factors. It could be that mutations to the *clpC* M-Domain might affect the forespore the way we expect, but they also cause unintended effects in the ClpC that is needed in the mother cell. To get around this, we propose to use two copies of the *clpC* gene: one that is expressed exclusively in the forespore through σ^F, and one that is expressed in the mother cell through all other sigma factors in the *ctsR* operon.

Current Camp Lab member Khushi Panchal has shown that the σ^F promoter can be knocked out of the *ctsR* operon with little reduction in spore formation ability, in addition to reducing ClpC significantly in the forespore and not the mother cell. If we inserted a second copy of *clpC* somewhere in the chromosome that has our M-Domain mutations in addition to a σ^F dependent promoter, we could potentially reduce the pleiotropic effects in the mother cell.

4.8.3 A proposal for further investigation into the F436 area on ClpC

Once we have determined how best to deal with the pleiotropic effects of ClpC, I want to propose another residue that I think could be interesting to explore. E183 is fairly well conserved in MdfA within the *Bacillaceae* family as primarily a glutamic acid (E, negatively charged) or glutamine (Q, polar uncharged) (Massoni et al. 2025). This residue is predicted to come in the most direct contact with F436, which as discussed earlier has important functions for adaptor

protein interactions (See Figure 4 & Figure 12). Through our experiments, we have seen that mutating *clpC*^{F436} to an alanine (A) is enough to break interaction between ClpC and MdfA; however, we have not tested this interaction from the MdfA side yet.

I am curious if this E183 residue on MdfA serves as an interaction point with F436 on ClpC, and if so, what kind of interaction does it have? As discussed, F436 on ClpC fits into a hydrophobic pocket on MecA to facilitate interaction, but MdfA lacks an obvious pocket that F436 could favorably sit in. I thought initially this interaction between F436 and E183 could be an example of an anion-π pairing interaction where the positively charged edge of an aromatic ring interacts with an anion to form an anion-quadrupole interaction, stabilizing intramolecular interactions (Philip et al. 2011); however, on further inspection of the predicted interface, it appears that the non-polar carbons on E183 sit parallel to the aromatic ring more than the charged head of glutamic acid. This could additionally explain why the other most commonly conserved form of the residue in the 183 position is glutamine, a non-polar, similarly sized amino acid to glutamic acid.

To determine if E183 is necessary for interaction with F436, and the ClpC M-Domain as a whole, I propose first to start by swapping E183 on MdfA to an alanine. Similar to our mutations made to *mdfA*^{E190}, I would expect this *mdfA*^{E183A} mutant to break interaction between ClpC and MdfA if E183 was an important partner to the F436 interface. Additionally, I would like to see what happens when E183 in *B. subtilis* is swapped to a glutamine, and if the similar structure to glutamic acid is able to rescue interaction, or if the lack of the polar head would disrupt interaction. In a similar fashion, could lucine (L, non-polar) that lacks any polar head group support interaction to F436 with a hydrophobic interaction?

There are a variety of amino acids that could be interesting to test and to simplify the number of mutations that would need to be made, we could use a larger screening method to determine what amino acid swaps would be worth pursuing. For this, we could attempt a method similar to a *E. coli* Bacterial 3-Hybrid (B3H) screening that has been used for work done by Stein et al. (2024). In short, the group was able to introduce different point mutations to the prey protein and then screen a number of amino acids at certain positions for their ability to bind with a given bait RNA. To rework this to align with our goals, we would use a B2H assay where a WT ClpC monomer would act as the bait and MdfA with a number of possible amino acids in the E183 position would be introduced. Colonies that have MdfA-ClpC interaction will appear blue while colonies with no or little interaction will appear white; these cells can then be sequenced to determine what amino acid took the place of E183 on MdfA.

REFERENCES

1. Annis, Marissa Y., Claire M. Ravenburg, and Klaas J. van Wijk. “Uvr Motifs Regulate the Chloroplast Clp Chaperone–Protease System.” *Trends in Plant Science* 0, no. 0 (October 24, 2024). https://doi.org/10.1016/j.tplants.2024.09.015.
2. Barboza, Perry S., Sean D. Farley, and Charles T. Robbins. “Whole-Body Urea Cycling and Protein Turnover during Hyperphagia and Dormancy in Growing Bears (Ursus Americanus and U. Arctos).” *Canadian Journal of Zoology* 75, no. 12 (December 1997): 2129–36. https://doi.org/10.1139/z97-848.
3. Camp, Amy H., and Richard Losick. “A Feeding Tube Model for Activation of a Cell-Specific Transcription Factor during Sporulation in Bacillus Subtilis.” *Genes & Development* 23, no. 8 (April 15, 2009): 1014–24. https://doi.org/10.1101/gad.1781709.
4. Camp, Amy H., Anna F. Wang, and Richard Losick. “A Small Protein Required for the Switch from σF to σG during Sporulation in Bacillus Subtilis.” *Journal of Bacteriology* 193, no. 1 (December 11, 2011): 116–24. https://doi.org/10.1128/jb.00949-10.
5. Carroni, Marta, Kamila B Franke, Michael Maurer, Jasmin Jäger, Ingo Hantke, Felix Gloge, Daniela Linder, et al. “Regulatory Coiled-Coil Domains Promote Head-to-Head Assemblies of AAA+ Chaperones Essential for Tunable Activity Control.” Edited by Andreas Martin. *eLife* 6 (November 22, 2017): e30120. https://doi.org/10.7554/eLife.30120.
6. Cutting, Simon, Scott Panzer, and Richard Losick. “Regulatory Studies on the Promoter for a Gene Governing Synthesis and Assembly of the Spore Coat in *Bacillus Subtilis*.” *Journal of Molecular Biology* 207, no. 2 (May 20, 1989): 393–404. https://doi.org/10.1016/0022-2836(89)90262-3.
7. Elsholz, Alexander K. W., Marlene S. Birk, Emmanuelle Charpentier, and Kürşad Turgay. “Functional Diversity of AAA+ Protease Complexes in Bacillus Subtilis.” *Frontiers in Molecular Biosciences* 4 (July 12, 2017). https://doi.org/10.3389/fmolb.2017.00044.
8. Evans, Richard, Michael O’Neill, Alexander Pritzel, Natasha Antropova, Andrew Senior, Tim Green, Augustin Žídek, et al. “Protein Complex Prediction with AlphaFold-Multimer.” bioRxiv, March 10, 2022. https://doi.org/10.1101/2021.10.04.463034.
9. González-Pastor, José E., Errett C. Hobbs, and Richard Losick. “Cannibalism by Sporulating Bacteria.” *Science* 301, no. 5632 (July 25, 2003): 510–13. https://doi.org/10.1126/science.1086462.

10. Hota, Susy S., Camille Achonu, Natasha S. Crowcroft, Bart J. Harvey, Albert Lauwers, and Michael A. Gardam. “Determining Mortality Rates Attributable to Clostridium Difficile Infection.” *Emerging Infectious Diseases* 18, no. 2 (February 2012): 305–7. https://doi.org/10.3201/eid1802.101611.
11. Kain, James, Gina G. He, and Richard Losick. “Polar Localization and Compartmentalization of ClpP Proteases during Growth and Sporulation in Bacillus Subtilis.” *Journal of Bacteriology* 190, no. 20 (October 15, 2008): 6749–57. https://doi.org/10.1128/jb.00589-08.
12. Khanna, Kanika, Javier Lopez-Garrido, and Kit Pogliano. “Shaping an Endospore: Architectural Transformations During Bacillus Subtilis Sporulation.” *Annual Review of Microbiology* 74, no. Volume 74, 2020 (September 8, 2020): 361–86. https://doi.org/10.1146/annurev-micro-022520-074650.
13. Kirstein, Janine, David A Dougan, Ulf Gerth, Michael Hecker, and Kürşad Turgay. “The Tyrosine Kinase McsB Is a Regulated Adaptor Protein for ClpCP.” *The EMBO Journal* 26, no. 8 (April 18, 2007): 2061–70. https://doi.org/10.1038/sj.emboj.7601655.
14. Kirstein, Janine, Tilman Schlothauer, David A Dougan, Hauke Lilie, Gilbert Tischendorf, Axel Mogk, Bernd Bukau, and Kürşad Turgay. “Adaptor Protein Controlled Oligomerization Activates the AAA+ Protein ClpC.” *The EMBO Journal* 25, no. 7 (April 5, 2006): 1481–91. https://doi.org/10.1038/sj.emboj.7601042.
15. Kroos, Lee, Bin Zhang, Hiroshi Ichikawa, and Yuen-Tsu Nicco Yu. “Control of σ Factor Activity during Bacillus Subtilis Sporulation.” *Molecular Microbiology* 31, no. 5 (1999): 1285–94. https://doi.org/10.1046/j.1365-2958.1999.01214.x.
16. Kuhlmann, Nathan J, and Peter Chien. “Selective Adaptor Dependent Protein Degradation in Bacteria.” *Current Opinion in Microbiology* 36 (April 2017): 118–27. https://doi.org/10.1016/j.mib.2017.03.013.
17. Leon, Ramon G., and Micheal D. K. Owen. “Regulation of Weed Seed Dormancy through Light and Temperature Interactions.” Accessed January 11, 2025. https://bioone-org.proxy.mtholyoke.edu:2443/journals/weed-science/volume-51/issue-5/P2002-173/Regulation-of-weed-seed-dormancy-through-light-and-temperature-interactions/10.1614/P2002-173.full.
18. Liu, Huanting, and James H. Naismith. “An Efficient One-Step Site-Directed Deletion, Insertion, Single and Multiple-Site Plasmid Mutagenesis Protocol.” *BMC Biotechnology* 8, no. 1 (December 4, 2008): 91. https://doi.org/10.1186/1472-6750-8-91.
19. Liu, Jing, Ziqing Mei, Ningning Li, Yutao Qi, Yanji Xu, Yigong Shi, Feng Wang, Jianlin Lei, and Ning Gao. “Structural Dynamics of the MecA-ClpC Complex: A Type II AAA+

Protein Unfolding Machine." *The Journal of Biological Chemistry* 288, no. 24 (June 14, 2013): 17597–608. https://doi.org/10.1074/jbc.M113.458752.

20. Mahmoud, Samar A, and Peter Chien. "Regulated Proteolysis in Bacteria." *Annual Review of Biochemistry* 87 (June 20, 2018): 677–96. https://doi.org/10.1146/annurev-biochem-062917-012848.
21. Massoni, Shawn C., Nicola J. Evans, Ingo Hantke, Colleen Fenton, James H. Torpey, Katherine M. Collins, Ewelina M. Krysztofinska, et al. "MdfA Is a Novel ClpC Adaptor Protein That Functions in the Developing Bacillus Subtilis Spore." *Genes & Development* 39, no. 7–8 (March 14, 2025): 510–23. https://doi.org/10.1101/gad.352498.124.
22. Meyer, Pablo, Jennifer Gutierrez, Kit Pogliano, and Jonathan Dworkin. "Cell Wall Synthesis Is Necessary for Membrane Dynamics during Sporulation of Bacillus Subtilis." *Molecular Microbiology* 76, no. 4 (2010): 956–70. https://doi.org/10.1111/j.1365-2958.2010.07155.x.
23. Morreale, Francesca E., Stefan Kleine, Julia Leodolter, Sabryna Junker, David M. Hoi, Stepan Ovchinnikov, Anastasia Okun, et al. "BacPROTACs Mediate Targeted Protein Degradation in Bacteria." *Cell* 185, no. 13 (June 23, 2022): 2338-2353.e18. https://doi.org/10.1016/j.cell.2022.05.009.
24. Nanamiya, Hideaki, Yoshiaki Ohashi, Kei Asai, Shigeki Moriya, Naotake Ogasawara, Masaya Fujita, Yoshito Sadaie, and Fujio Kawamura. "ClpC Regulates the Fate of a Sporulation Initiation Sigma Factor, σH Protein, in Bacillus Subtilis at Elevated Temperatures." *Molecular Microbiology* 29, no. 2 (1998): 505–13. https://doi.org/10.1046/j.1365-2958.1998.00943.x.
25. Pan, Qi, Danielle A. Garsin, and Richard Losick. "Self-Reinforcing Activation of a Cell-Specific Transcription Factor by Proteolysis of an Anti-σ Factor in B. Subtilis." *Molecular Cell* 8, no. 4 (October 26, 2001): 873–83. https://doi.org/10.1016/S1097-2765(01)00362-8.
26. Pan, Stefan, Aaron A. Jensen, Nicholas A. Wood, Beate Henrichfreise, Heike Brötz-Oesterhelt, Derek J. Fisher, Peter Sass, and Scot P. Ouellette. "Molecular Characterization of the ClpC AAA+ ATPase in the Biology of Chlamydia Trachomatis." *mBio* 14, no. 2 (March 28, 2023): e00075-23. https://doi.org/10.1128/mbio.00075-23.
27. Philip, Vivek, Jason Harris, Rachel Adams, Don Nguyen, Jeremy Spiers, Jerome Baudry, Elizabeth E. Howell, and Robert J. Hinde. "A Survey of Aspartate−Phenylalanine and Glutamate−Phenylalanine Interactions in the Protein Data Bank: Searching for Anion−π Pairs." *Biochemistry* 50, no. 14 (April 12, 2011): 2939–50. https://doi.org/10.1021/bi200066k.

28. Riley, Eammon P., Jelani A. Lyda, Octavio Reyes-Matte, Joseph Sugie, Iqra R. Kasu, Eray Enustun, Emily Armbruster, et al. “Developmentally-Regulated Proteolysis by MdfA and ClpCP Mediates Metabolic Differentiation during Bacillus Subtilis Sporulation.” bioRxiv, November 26, 2024. https://doi.org/10.1101/2024.11.26.625531.
29. Riley, Eammon P., Corinna Schwarz, Alan I. Derman, and Javier Lopez-Garrido. “Milestones in Bacillus Subtilis Sporulation Research.” *Microbial Cell* 8, no. 1 (n.d.): 1–16. https://doi.org/10.15698/mic2021.01.739.
30. Sachla, Ankita J., Alexander J. Alfonso, and John D. Helmann. “A Simplified Method for CRISPR-Cas9 Engineering of Bacillus Subtilis.” *Microbiology Spectrum* 9, no. 2 (September 15, 2021): e00754-21. https://doi.org/10.1128/Spectrum.00754-21.
31. Sauer, R. T., & Baker, T. A. (2011). AAA+ proteases: ATP-fueled machines of protein destruction. Annual review of biochemistry, 80, 587–612.
32. Schumann, Wolfgang. “Regulation of Bacterial Heat Shock Stimulons.” *Cell Stress and Chaperones* 21, no. 6 (November 1, 2016): 959–68. https://doi.org/10.1007/s12192-016-0727-z.
33. Tan, Irene S., and Kumaran S. Ramamurthi. “Spore Formation in Bacillus Subtilis.” *Environmental Microbiology Reports* 6, no. 3 (2014): 212–25. https://doi.org/10.1111/1758-2229.12130.
34. Trentini, Débora Broch, Marcin Józef Suskiewicz, Alexander Heuck, Robert Kurzbauer, Luiza Deszcz, Karl Mechtler, and Tim Clausen. “Arginine Phosphorylation Marks Proteins for Degradation by a Clp Protease.” *Nature* 539, no. 7627 (November 2016): 48–53. https://doi.org/10.1038/nature20122.
35. Turgay, K., L. W. Hamoen, G. Venema, and D. Dubnau. “Biochemical Characterization of a Molecular Switch Involving the Heat Shock Protein ClpC, Which Controls the Activity of ComK, the Competence Transcription Factor of Bacillus Subtilis.” *Genes & Development* 11, no. 1 (January 1, 1997): 119–28. https://doi.org/10.1101/gad.11.1.119.
36. Turgay, Kürşad, Jeanette Hahn, Jan Burghoorn, and David Dubnau. “Competence in Bacillus Subtilis Is Controlled by Regulated Proteolysis of a Transcription Factor.” *The EMBO Journal* 17, no. 22 (November 16, 1998): 6730–38. https://doi.org/10.1093/emboj/17.22.6730.
37. Wang, Feng, Ziqing Mei, Yutao Qi, Chuangye Yan, Qi Hu, Jiawei Wang, and Yigong Shi. “Structure and Mechanism of the Hexameric MecA–ClpC Molecular Machine.” *Nature* 471, no. 7338 (March 2011): 331–35. https://doi.org/10.1038/nature09780.
38. Wu, Ling Juan, and Jeffery Errington. “Use of Asymmetric Cell Division and spoIIIE Mutants to Probe Chromosome Orientation and Organization in Bacillus Subtilis.”

Molecular Microbiology 27, no. 4 (1998): 777–86. https://doi.org/10.1046/j.1365-2958.1998.00724.x.